

# Summary of WG4

## Applications of High Brightness Beams to Advanced Accelerators and Light Sources

Chaired by Mitsuru Uesaka ( Univ.Tokyo)  
Scientific secretary: Andrea Rossi ( Univ.Milan)

1. Compton Scattering X-ray Sources
2. FEL and RF Photoinjectors
3. Plasma Wakefield Acceleration and Innovative Acceleration Schemes

16 contributions

# Compton Scattering X-ray Sources

## 1. Multi-Scattering for More Yield and Medical Applications

Mitsuru Uesaka(Univ.Tokyo)

“Medical Application of Multi-beams Compton Scattering Monochromatic Tunable Hard X-ray Sources”

Haruyuki Ogino(Univ.Tokyo)

“Laser Pulse Circulation System for Compact Monochromatic Hard-X-Ray Source”

## 2. Strong Focusing and Higher Harmonics Generation

Jae Lim(LLNL)

“A permanent –Magnet Quadrupole Final focusing Optics at PLEIADES Thomson X-ray Source”

Oliver Williams(UCLA)

“Status of the Nonlinear Inverse Compton Scattering Experiment at UCLA”

Rodney Yoder(Manhattan College)

“An Inverse Compton Scattering Radiation Source via Self-Guiding in a Plasma”

Vitaly Yakimenko(BNL)

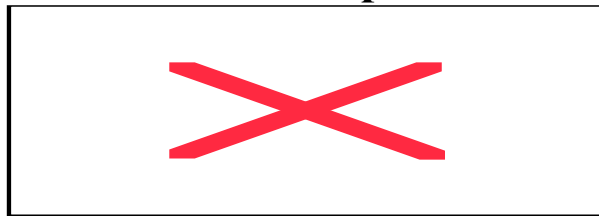
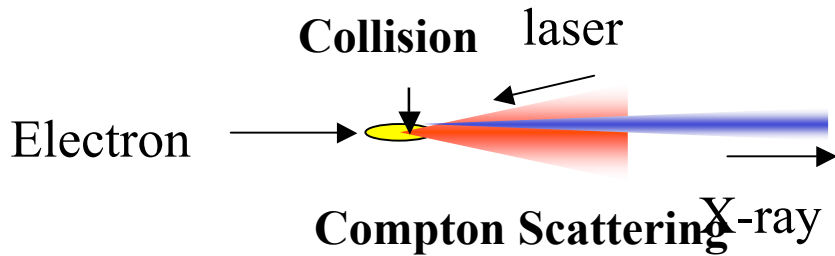
“Nonlinear Compton Scattering at BNL-ATF”

## 3. Theory and simulation

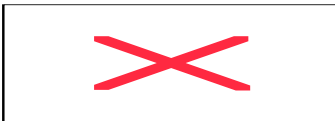
Vittoria Petrillo(Univ.Milan)

“Study of transverse effects in a collective Thomson Back-scattering Source of X-rays”

# Monochromatic Hard X-ray by Compton Scattering

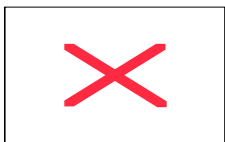
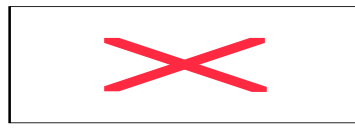
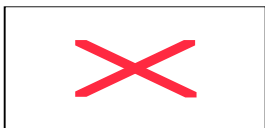


( $K$ : Wiggling angle of electron)

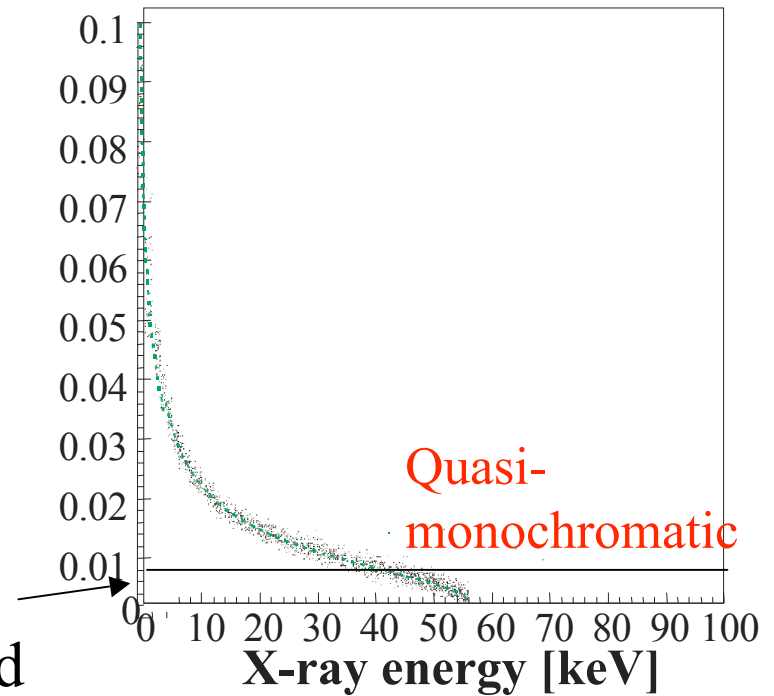


(laser wavelength)

5mrad



(X-ray)

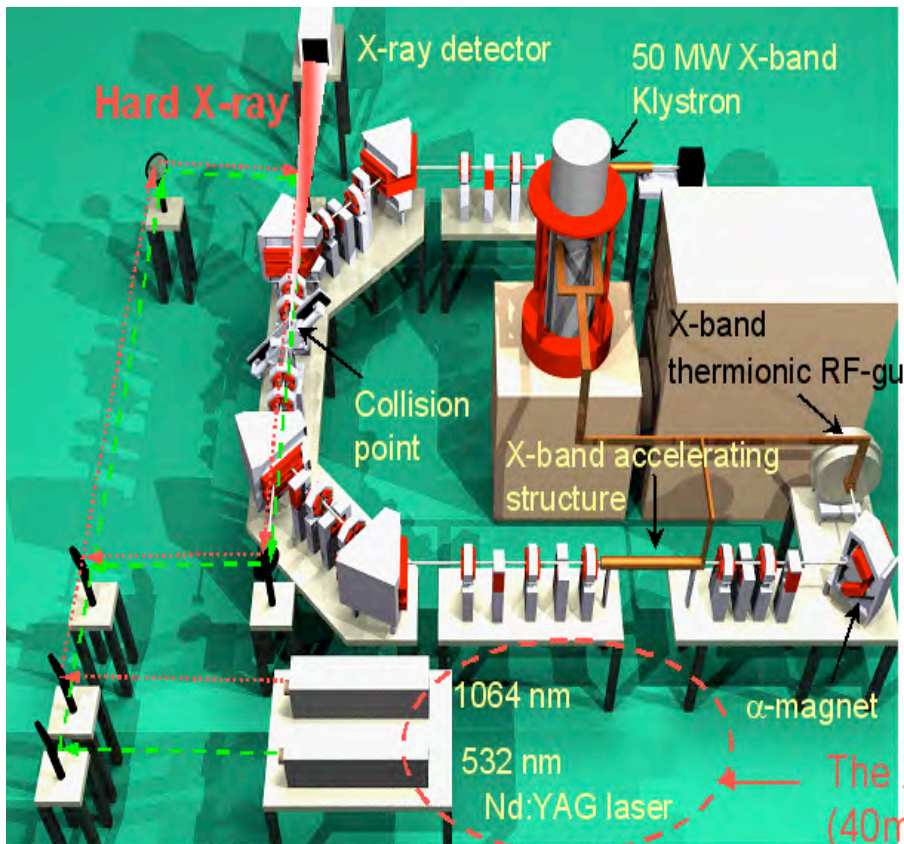


X-ray energy vs Angle

# Compton scattering hard X-ray source

Compact hard X-ray source based on Compton Scattering

Properties of the generated X-ray



Electron beam energy : 35 MeV, Charge : 20 pC/bunch

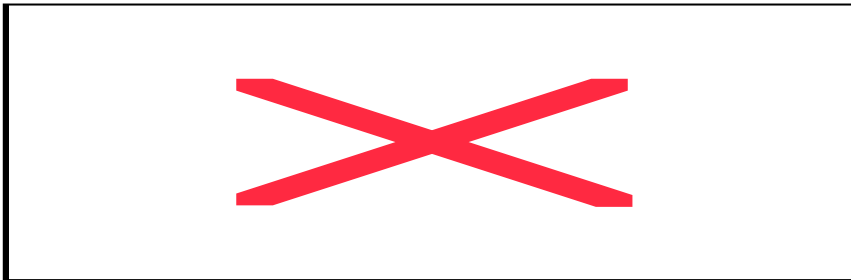
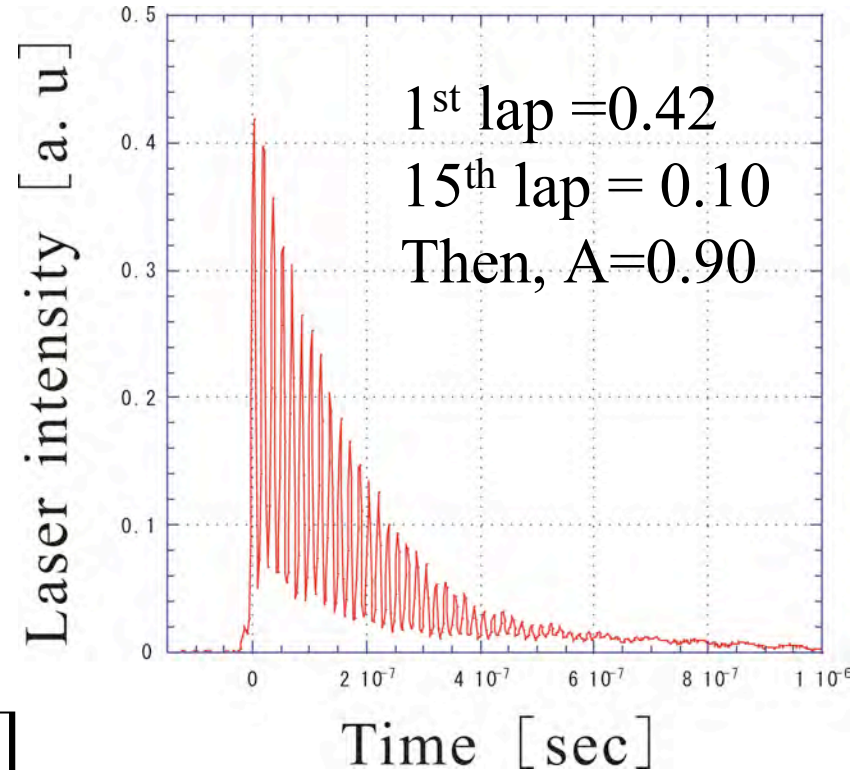
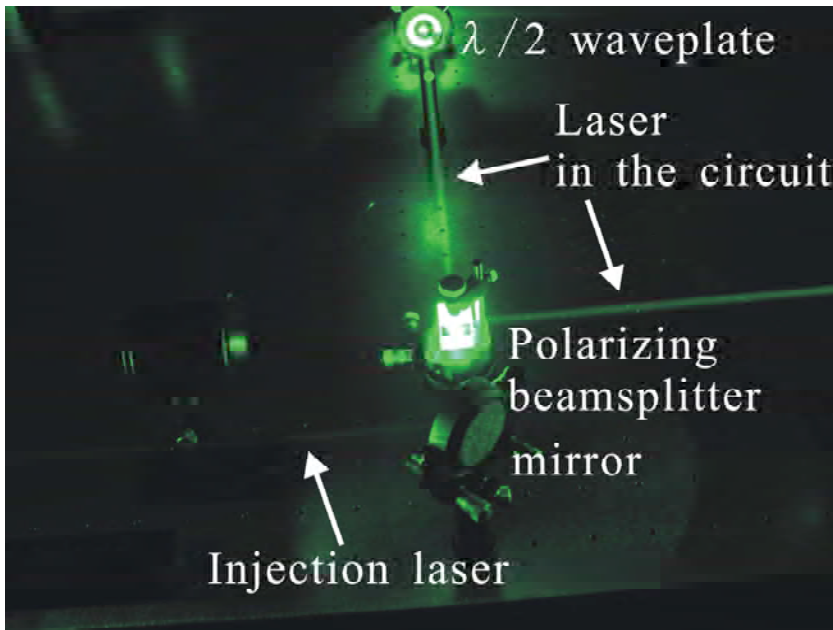
Laser wavelength (nm)	1064	532
Pulse energy (J/pulse)	2.5	1.4
X-ray yield (photons/pulse)	$9.9 \times 10^6$ ( $10^8$ )	$4.4 \times 10^6$ ( $10^8$ )
Maximum X-ray energy (keV)	21.9	43.8
Energy spread (%) rms	1-10	

Details are in RPAP006 and WPAP019

10 pps with laser circulation

The X-ray energy can be changed quickly (40ms) by introducing two lasers

# LPCS experiment result, longitudinal direction



A=0.90, n=50

Then, 10times higher intensity

$I_0$ : Incident laser pulse energy.

$I_n$ : Laser intensity in the laser pulse circulation system.

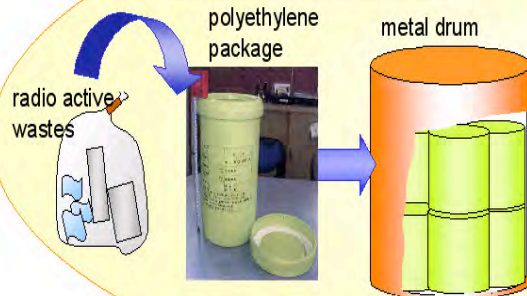
A: Transmission efficiency per one cycle.

n: Total number of the collisions.

# Application plans of the compact hard X-ray source

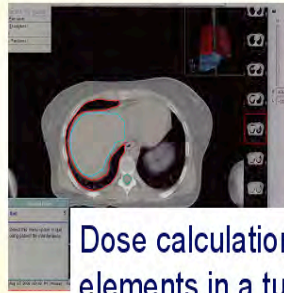
## Atomic number identification by dual-energy X-ray CT

### Nondestructive test



Element analysis inside a package

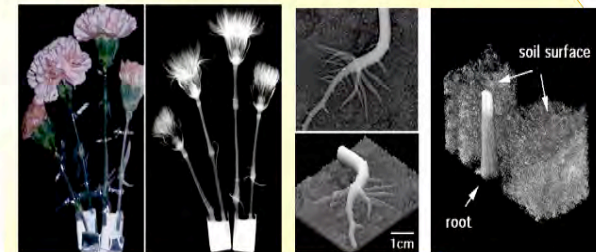
### Radiation Treatment Planning



Dose calculation by considering elements in a tumor for advanced radiation therapy

### Neutron radiography with X-ray CT

Imaging of water in a plant [3,4]

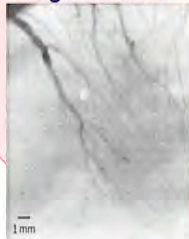


Movement of a element in a living plant

## Compact monochromatic hard X-ray source

### Micro vessel angiography

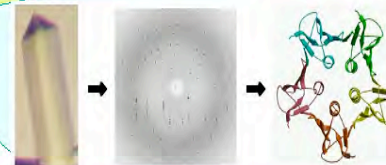
Image of coronary [5]



Diameter of micro vessel is less than  $100\mu\text{m}$

Micro vessel angiography will be tested with spatial resolution of  $100\mu\text{m}$

### Protein structural analysis



Structure analysis in a small laboratory

# Status of the Nonlinear ICS Experiment at UCLA

Oliver Williams  
UCLA Dept. Of Physics and Astronomy  
Erice, Sicily  
October 9-14 2005

# Beam Parameters

Parameter	Value
Electron Beam Energy	14 MeV
Beam Emittance	5 mm-mrad
*Electron Beam Spot Size (RMS)	25 $\mu\text{m}$
Beam Charge	300 pC
Bunch Length (RMS)	4 ps
*CO <sub>2</sub> Laser beam waist at IP	25 $\mu\text{m}$
*Laser wavelength	10.6 $\mu\text{m}$
*Laser Rayleigh Range	0.75 mm
*Laser Power	500 GW
Laser Pulse Length	200 ps

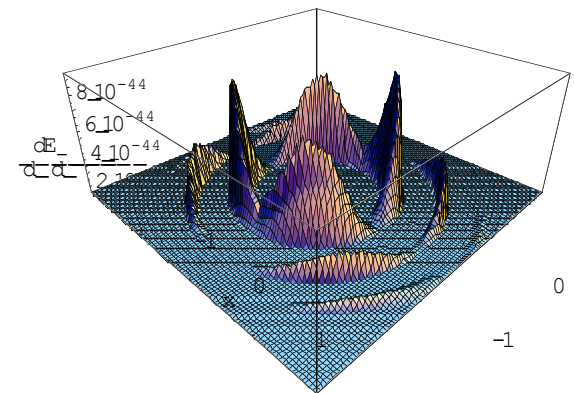
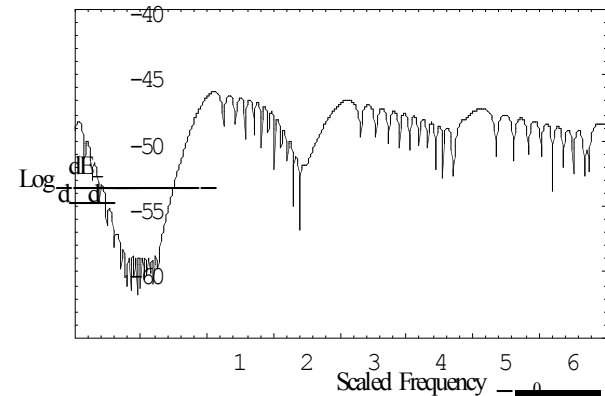


Laser guiding in plasma might be an option to increase interaction time and hence ICS photon flux (see talk by R. Yoder)



# Expected Spectrum and Intensity Distributions

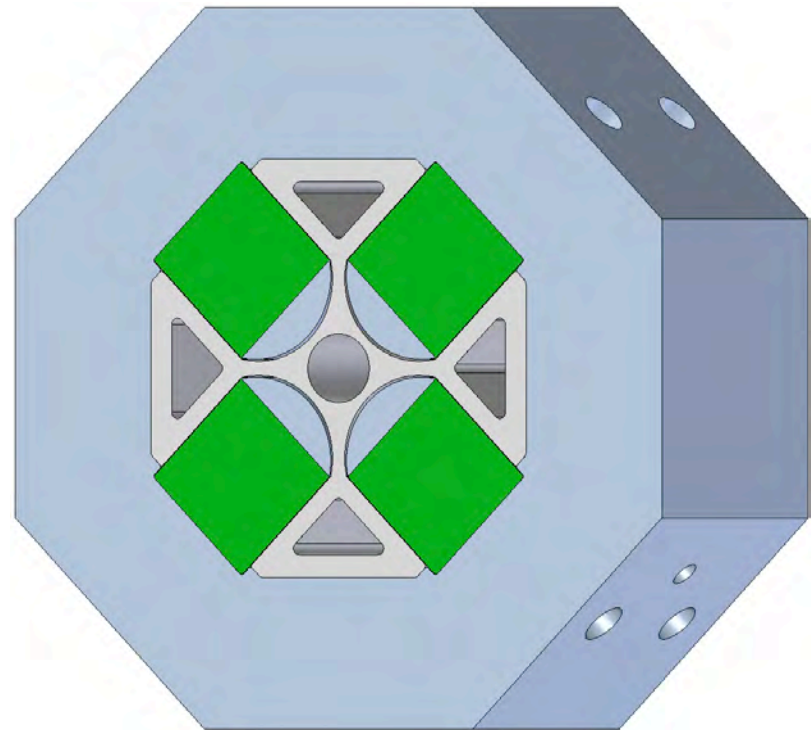
- Spectral broadening of the ICS photons is expected due to the ponderomotive scattering of the electrons from high laser field
- Even AND odd harmonics are expected to be prevalent off-axis
- Shown are frequency and intensity ( $2^{\text{nd}}$  harmonic) distributions seen on axis of the ICS photons for a  $\sigma$ -polarized, incident gaussian laser profile



Courtesy of A. Doyuran and G. Krafft

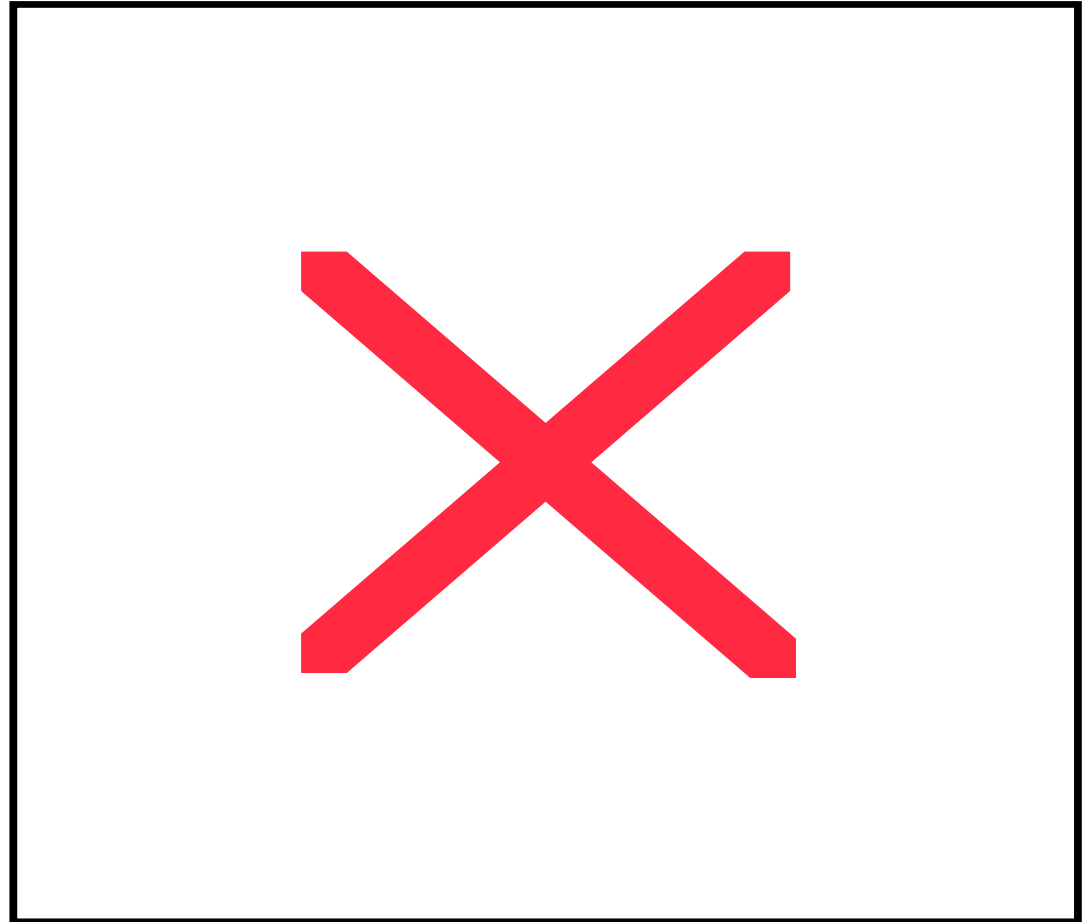
# PMQ Performance

- Measured  $\sim 110$  T/m focusing gradient of PMQ's
- Obtained a  $40\text{-}50 \mu\text{m}$   $\sigma_{x,y}$  RMS beam at the IP
- Measurements at only 38.5 kV in the modulator, corresponding to a  $\sim 12.5$  MeV beam
- Emittance expected to be less than optimal due to low field on cathode and asymmetric laser profile
- PMQ spacing and gradient optimized for 14 MeV beam, therefore smaller spots expected in future with emittance improvement and higher energy electrons

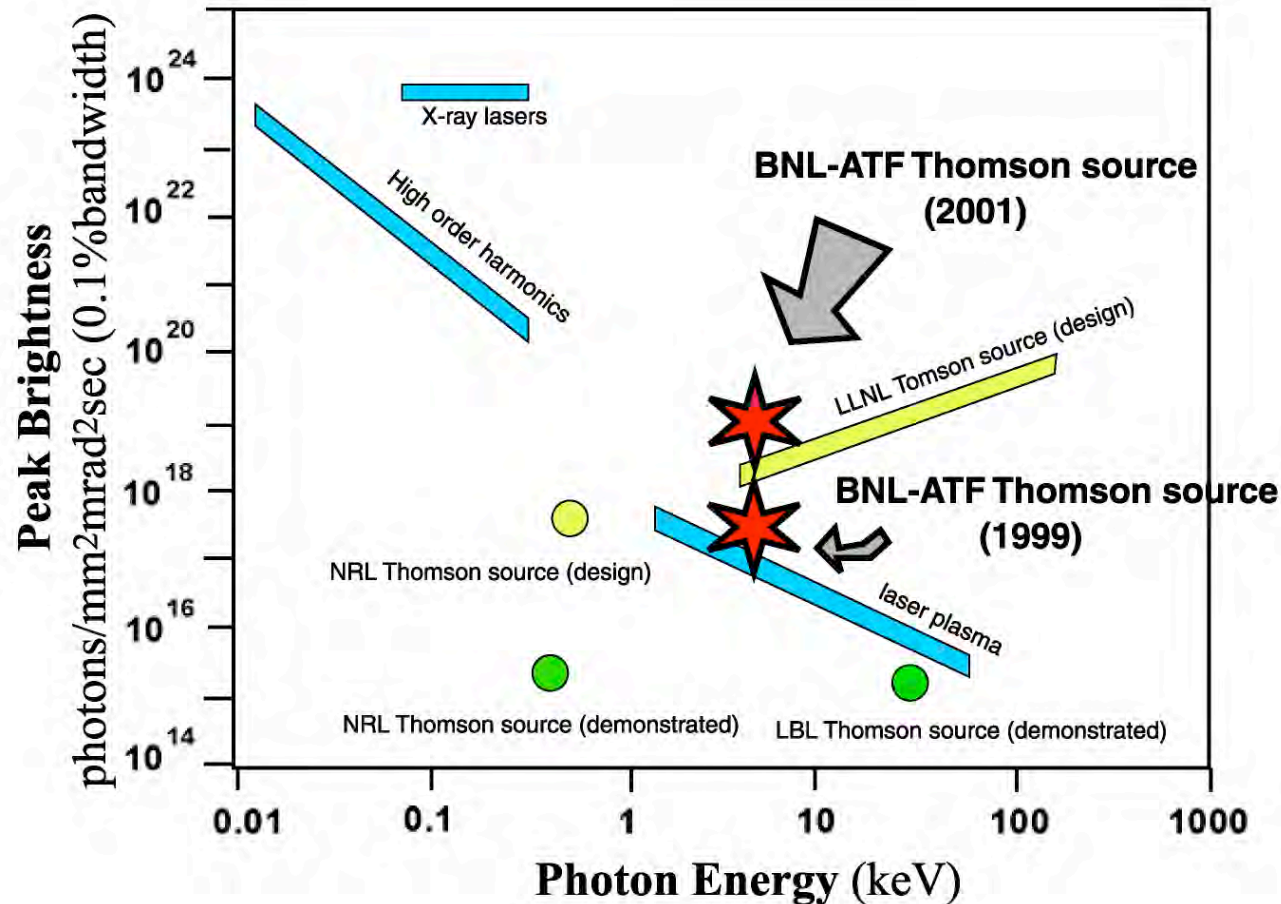


# Initial Alignment/Synchronization Results

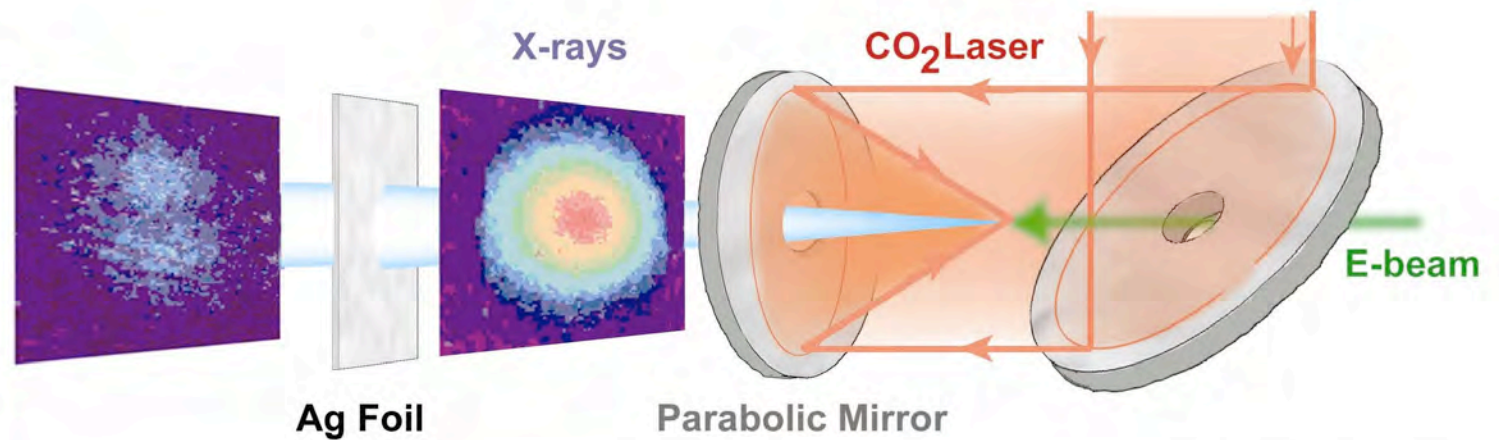
- Initial alignment done using graphite-coated phosphor
- Synchronization achieved using Ge crystal acting as a “gate” to 10.6  $\mu\text{m}$  radiation, where e-beam is the “key”
- 10.6  $\mu\text{m}$  absorbing semiconductor plasma created with formation length approx. e-beam bunch length
- Limits resolution to  $\sim 10$  ps (but have 200 ps laser pulse)
- This method requires spatial overlap, therefore confident beams are “seeing” each other



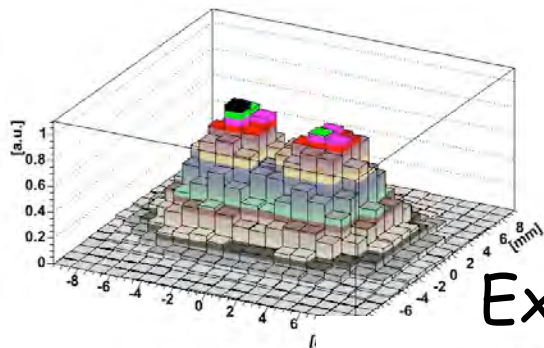
# Compton Scattering of Picosecond Electron and CO<sub>2</sub> Laser Beams



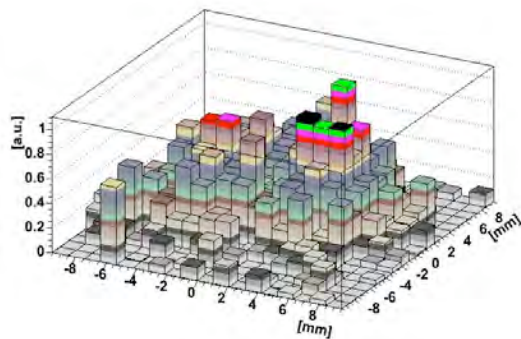
# Nonlinear Compton Scattering at ATF, Brookhaven (submitted to PRL)



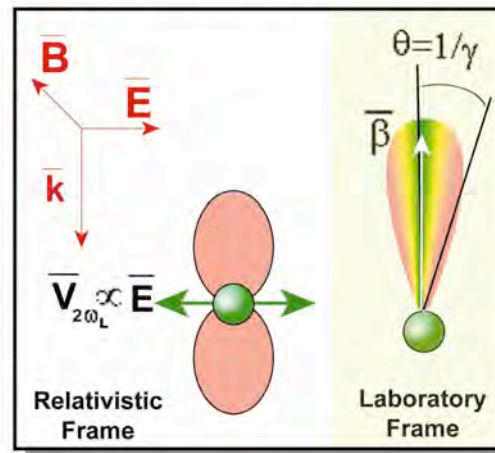
## Simulations



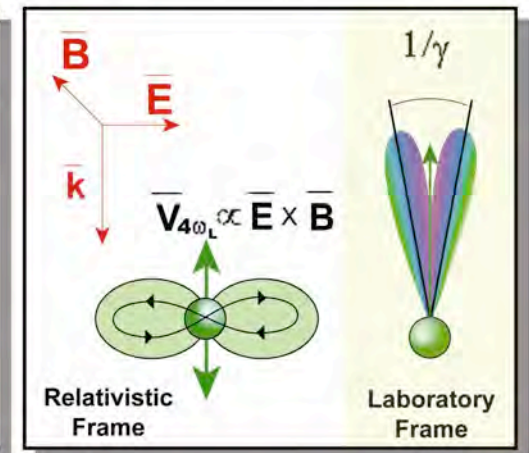
## Experiment



### First Order Fundamental Radiation



### Second Order Harmonic Radiation



# Study of transverse effects in a back-scattering coherent Thomson source of X-rays

A.Bacci, M.Ferrario\*,

C. Maroli, V.Petrillo, A.Rossi, L.Serafini

Università e Sezione I.N.F.N. di Milano (Italy)

\*LNF, Frascati (Italy)

If the laser pulse is long enough, **collective effects** can develop.  
The system electron beam + laser pulse behaves like a **free-electron laser with an electromagnetic wiggler**.

J. Gea-Banacloche, G. T. Moore, R.R. Schlicher, M. O. Scully, H. Walther, IEEE Journal of Quantum Electronics, QE-23, 1558 (1987).

B.G.Danly, G.Bekefi, R.C.Davidson, R.J.Temkin,T.M.Tran,J.S.Wurtele, IEEE Journ. of Quantum Electronics, QE-23,103(1987).

Gallardo, J.C., Fernow, R.C., Palmer, R., C. Pellegrini, IEEE Journal of Quantum Electronics 24, 1557-66 1988.

In particular, if the time duration of the laser pulse  $\Delta T_L$  is larger than a few gain lengths, i.e. if

$$\Delta T_L > (10) L_g/c$$

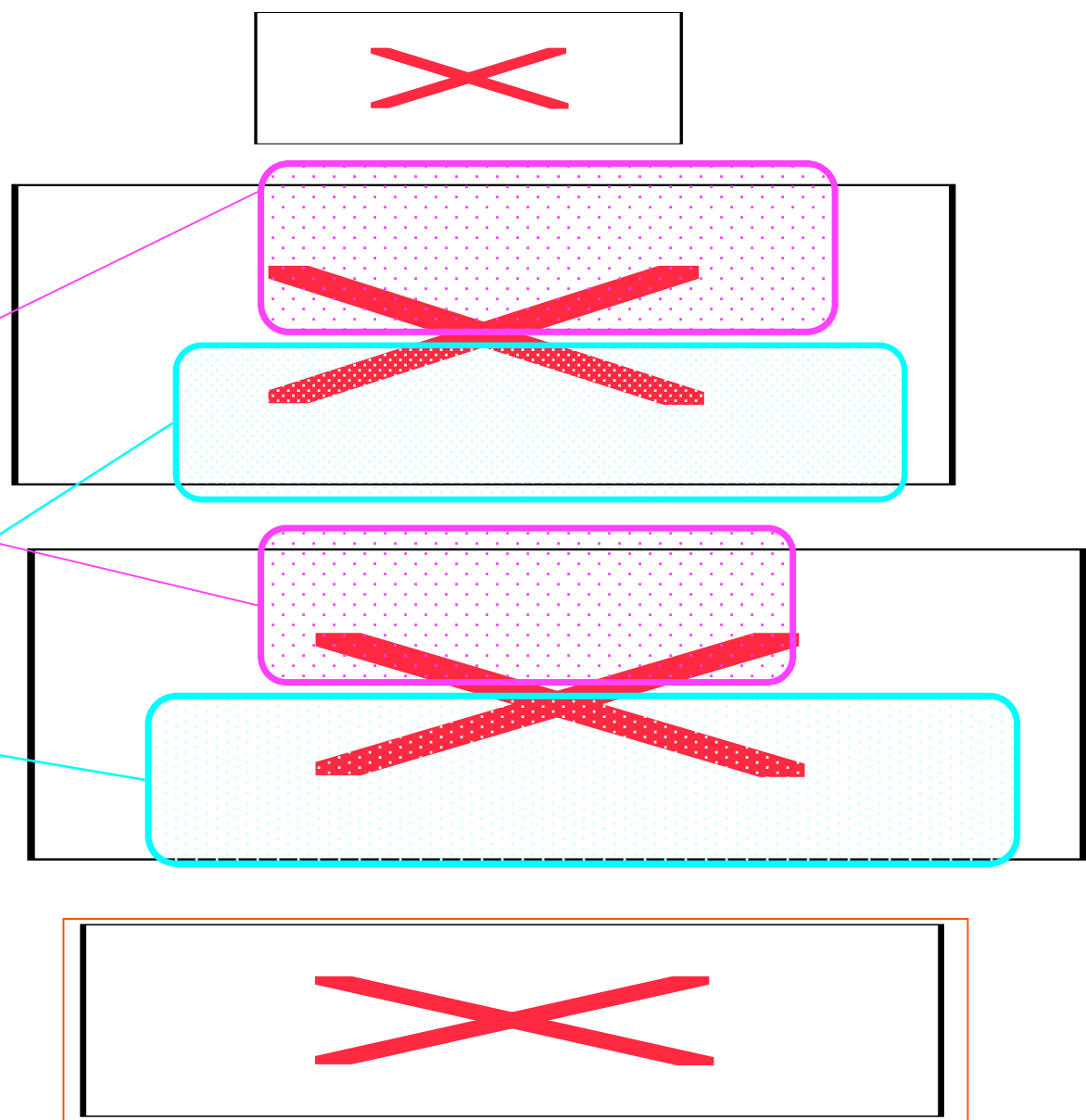
the electron of the beam can bunch and the f.e.l. instability can develop.

The coherent radiation is expected to have a spectrum bandwidth very much narrower than the incoherent radiation, a less broad angular distribution and (if the saturation is reached) a larger intensity.

Electron equations

Collective ponderomotive effects

Radiation equation





**Laser pulse:** time duration up to 5 psec power 1-3 TW, varying  $w_0$ ,  
 $\lambda=0,8-1$  micron

**Electron beam counterpropagating respect the laser pulse**

$Q=1\text{nC}$ ,  $l_b=100-300\text{micron}$ , radius  $\sigma_0=10-20$  micron,  $I=1-2,5$  KA

Energy=15 MeV ( $\gamma=30$ ), transverse norm emittance up to 3 mm mrad,  
 $\delta\gamma/\gamma=10^{-4}$ .

$$\rho=5 \cdot 10^{-4}$$

gain length

$$L_g= 100-150 \text{ micron}$$

**Radiation**

$$\lambda=3,5 \text{ Ang}$$

$$Z_R=1-4\text{m}$$

$\rho_{\text{bar}}=2 \rightarrow$  no quantum effects

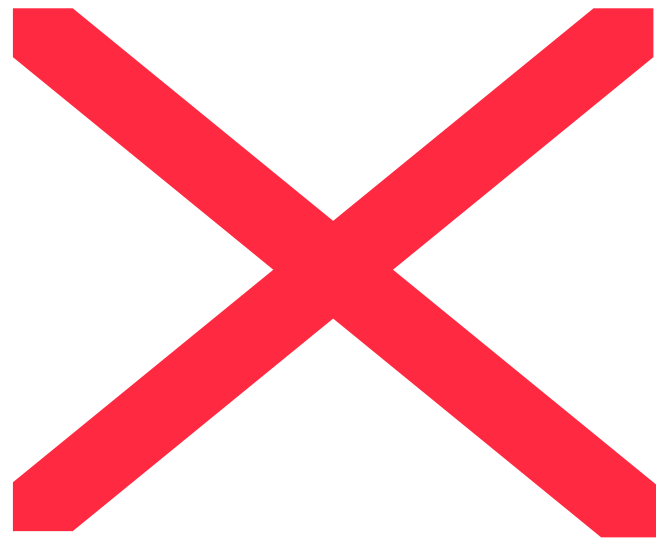
Transverse radiation intensity  
for emittance=1.8

t=1 ps

t=2 psec

t=3 ps

t=4 ps



Initially more chaotic, then smoother

## Conclusions

The growth of collective effects in the back scattering Thomson process is possible provided that:

A low-energy , high-brightness electron beam is available with short gain length

The optical laser pulse is long enough to permit the bunching and the instauration of the instability.

In the interaction region the laser transverse and longitudinal profiles are flat.



# **A Permanent-Magnet Quadrupole Final-Focusing Optics at PLEIADES Inverse Compton X-ray Source**



J. K. Lim\*, P. Frigola, J. B. Rosenzweig  
& G. Travish (UCLA)



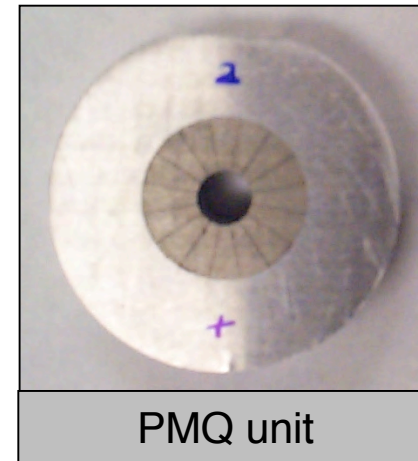
S. G. Anderson, D. J. Gibson, F. V. Hartemann  
& A. M. Tremaine (LLNL)

\* [jlim@physics.ucla.edu](mailto:jlim@physics.ucla.edu)

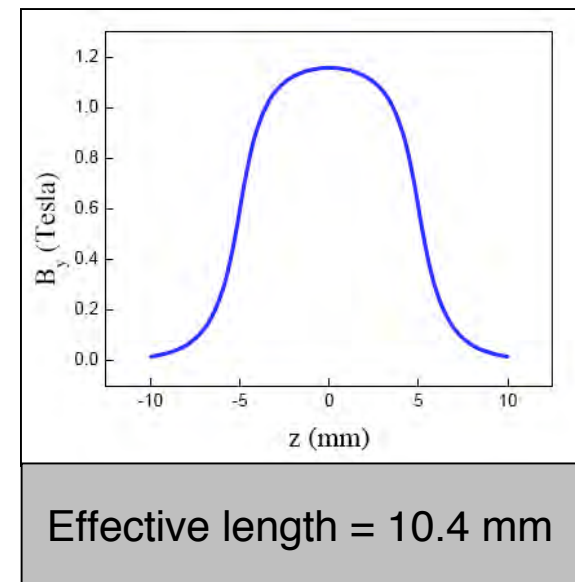
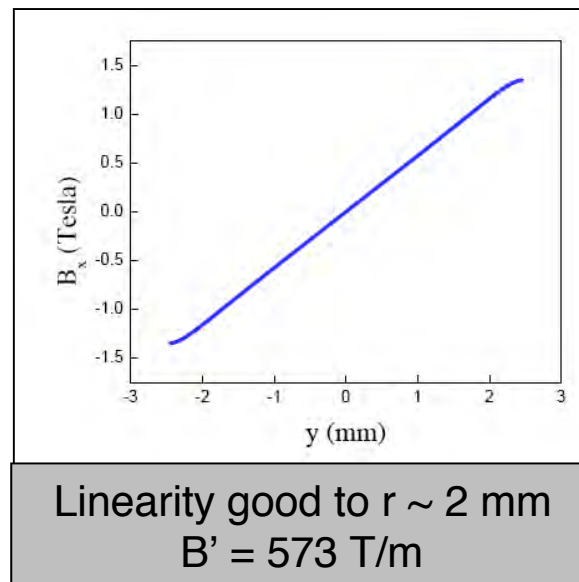
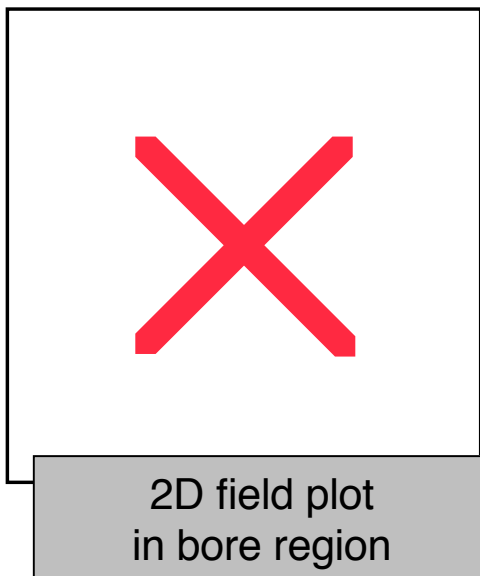
# High-field Gradient obtained from PMQ

$$B' = 2B_r \left( \frac{1}{r_i} - \frac{1}{r_o} \right)$$

For  $r_i=7.5\text{mm}$ ,  $r_o=5\text{mm}$  and  $B_r=1.2\text{T}$   
Field gradient of idealized PMQ is  
**640T/m**

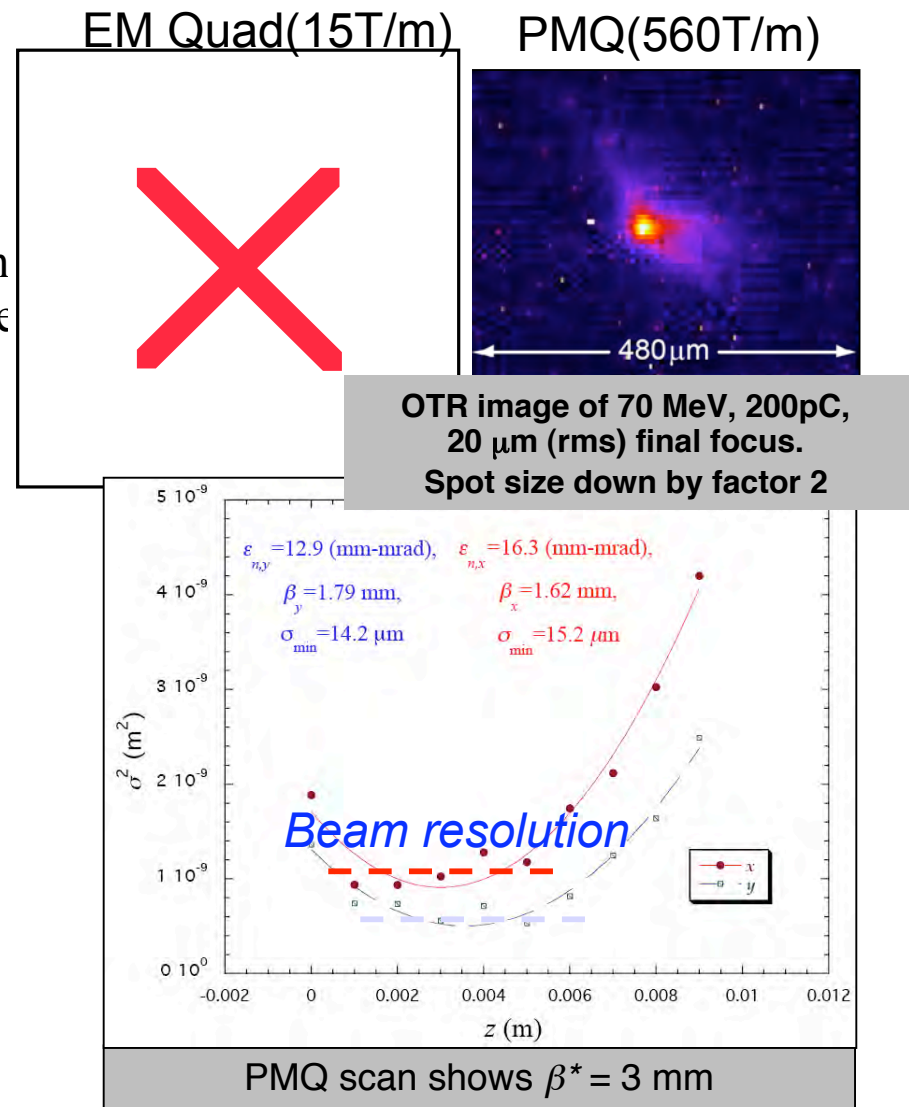


RADIA – 3D magnet simulation:



# Final focus performance is enhanced with PMQ system

- Final focus procedure:
  - Twiss parameters obtain from quad scan with up-stream magnets
  - Use Trace3D to compute EM quad setting  $\sim$  few meter  $\beta_0$  and PMQ positions for beam focus
- IP spot measured with OTR + 3  $\mu\text{m}/\text{pixel}$  video camera
  - $< 20 \mu\text{m}$  spots directly measured
  - Beam image aberration problem?
- PMQ scan analysis indicates  $\sigma^* = 15 \mu\text{m}$



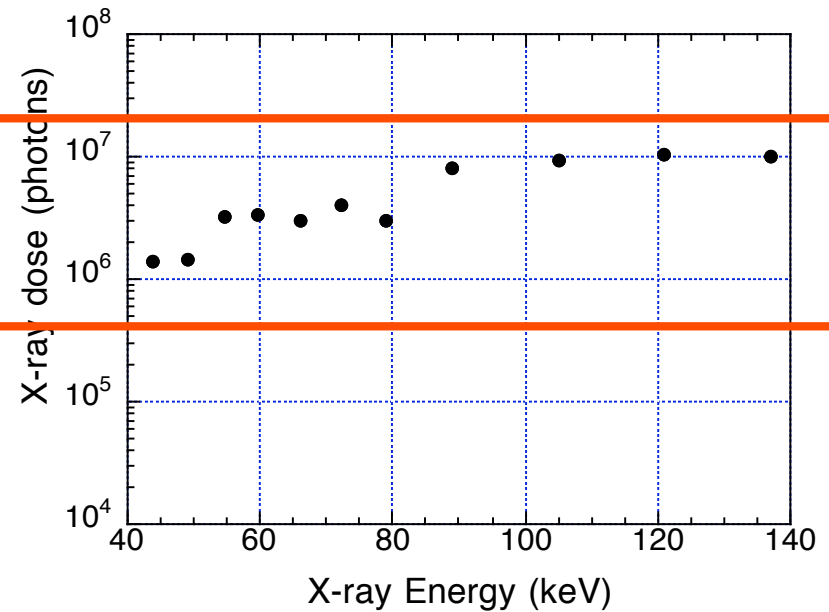
# The PLEIADES energy-tunable x-ray source

- Tunable, bright, ICS hard x-ray source
- 810 nm, 250 mJ, 54 fsec, Ti:Sapphire laser
- Under 20 micron beam spotsize w/ PMQ at ICS interaction

## RF Gun+LINAC

- 100 MeV/m
- Charge = 0.3 nC
- $\epsilon_n = 5$  mm-mrad
- $f = 2.85$  GHz (S-Band)
- $E = 20 - 100$  MeV
- ┌  $\sigma_t = 3$  ps (uncompressed)
- ┌  $\sigma_t < 300$  fs (compressed)

X-ray flux vs. energy



PMQ FINAL FOCUSING LENS  
has significantly increased source  
flux and brightness.



# An Inverse-Compton- Scattering Source via Self- Guiding in a Plasma

R. B. Yoder

*Manhattan College, New York*

J. B. Rosenzweig

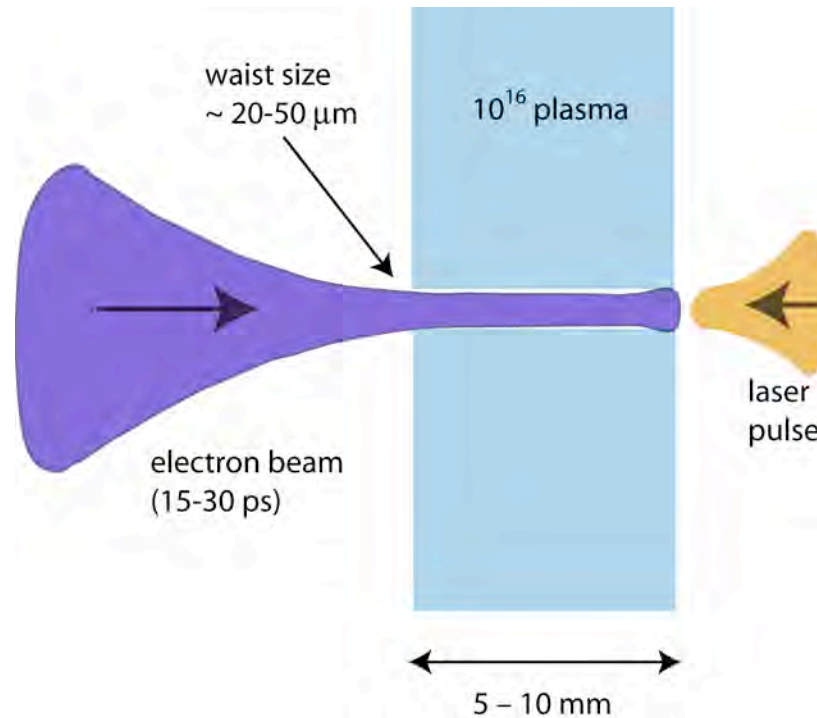
*UCLA Dept. of Physics and Astronomy*

ICFA Workshop on High-Brightness  
Beams,

Erice, October 2005



# Beam-driven channel scenario

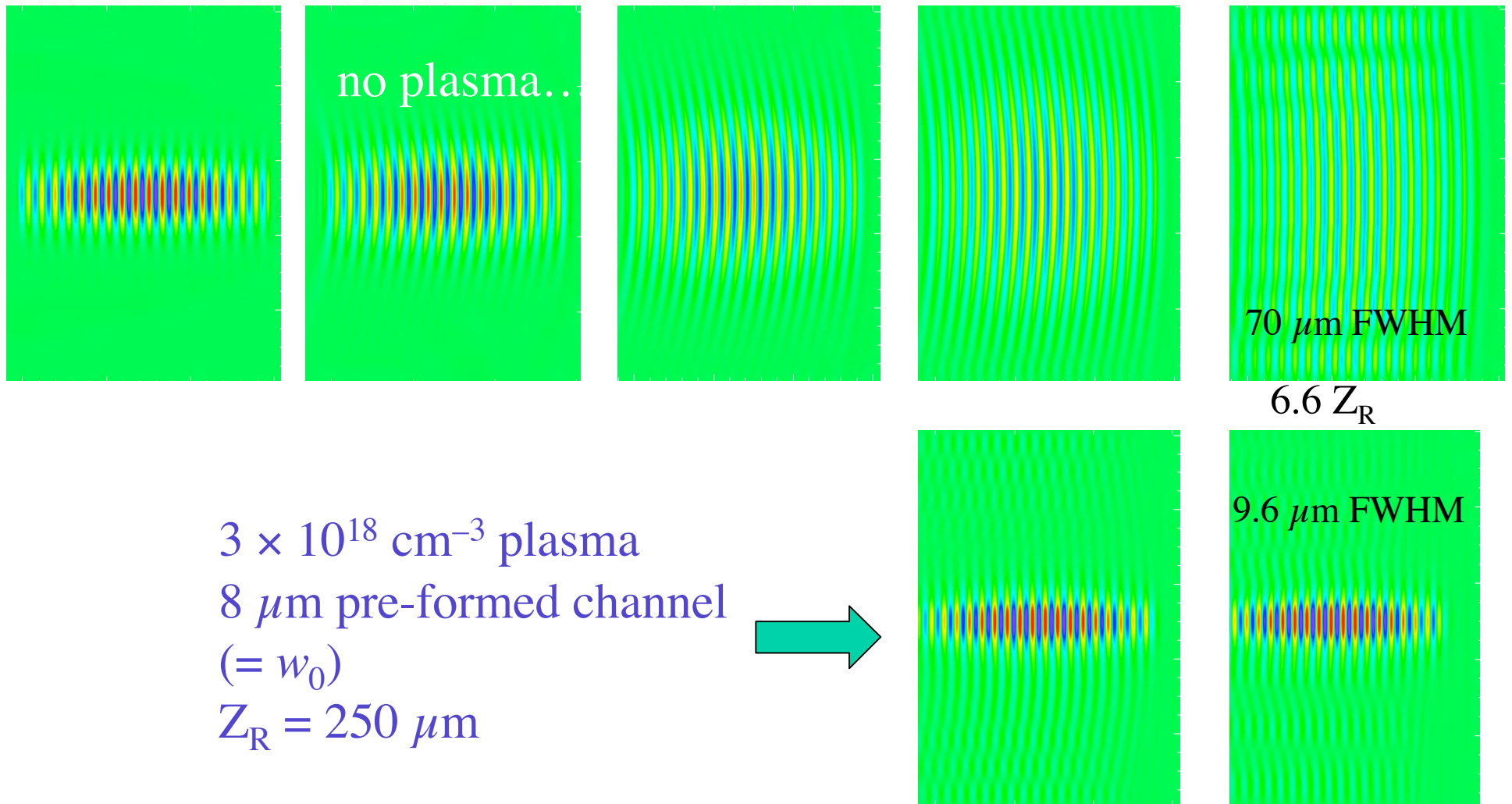


- long electron beam (3–4 mm), high charge (~10-100 nC)
- laser pulse arrives when beam head exits plasma
- laser guiding over 5–10  $Z_R$  through plasma-formed channel

R.Yoder and J.Rosenzweig

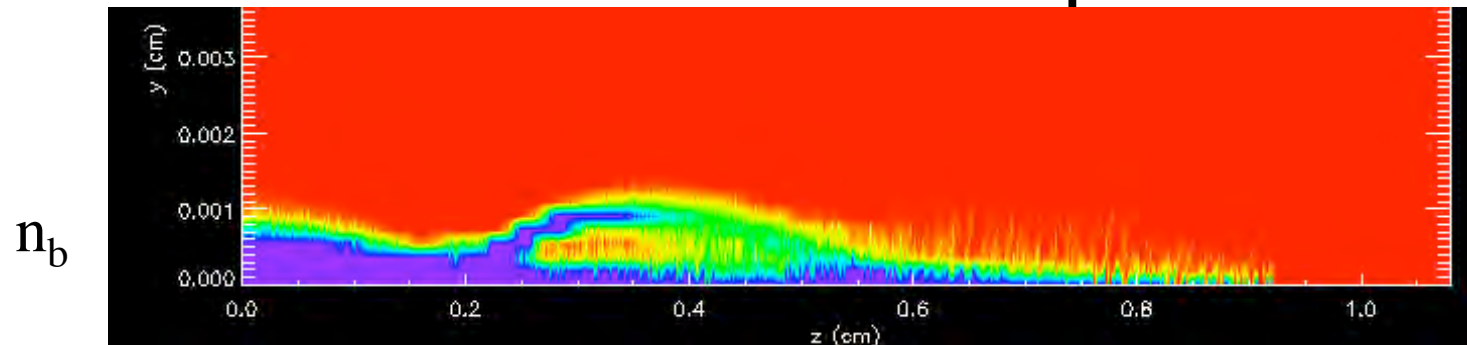
# Laser guiding: 2D simulation

800 nm, 50 fs pulse

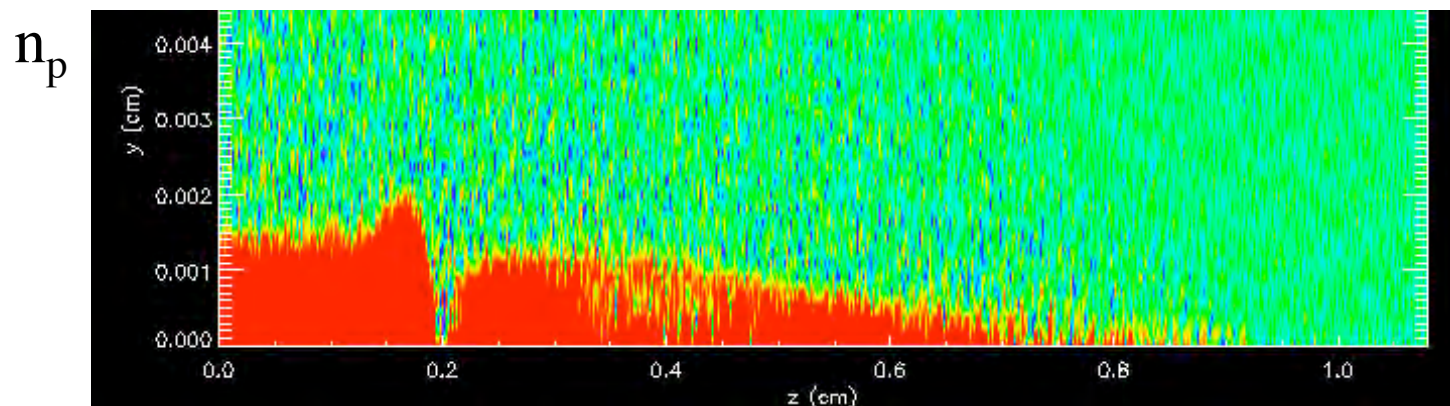


# Plasma channel formation

$t = 300 \text{ ps}$



self-pinching (overfocusing)



10 nC beam  
1.6 GeV  
 $5 \mu\text{m } \sigma_r$   
 $3 \text{ mm } \sigma_z$   
 $27 \text{ mm mrad } \epsilon_n$

Spectral order; red = 0

# Projected Photon Flux

Approximately: 
$$N_x = \sigma_T \frac{N_b N_\gamma}{A} f$$

$A$  is transverse overlap area;  $f$  is ratio of lengths ( $\leq 1$ );  
 $\sigma_T = 0.6$  barn

Assume 800 nm laser, 1 TW, 500 fs, 20  $\mu\text{m}$  spot:

-  $N_\gamma \sim 10^{18}$ ,  $N_b = 6 \times 10^{11}$ , entire laser pulse is usable energy,  $a_L < 0.1$

⇒ photon yield roughly  $10^9 - 10^{10}$  / pulse

With 10.6  $\mu\text{m}$ ,  $N_\gamma$  goes up, but  $a_L \sim 0.5 - 1$

*Very challenging simulation problem!*

- resolve laser wavelength over  $\sim 10Z_R = 3000 \lambda$
- symmetry problem: e-beam cylindrical, laser Cartesian

# Conclusion

- Self-guiding in plasma by electron beam has potential to create a high-brightness, long-pulse x-ray source through inverse Compton scattering

- *conceptually simple*
- *easy to time*
- *high photon number output*

- Output looks competitive with other x-ray and  $\gamma$ -ray generation methods involving pre-formed channels or multiple lasers

- **Not** necessary to use 10.6  $\mu\text{m}$  laser!
  - increase in photon number offset by high  $a_L$
  - similar performance from 800nm systems
- Simulation of yield is tough — ongoing project

# Summary of Compton Scattering X-ray Sources

1. **Multi-scattering system** to increase the X-ray yield has been proposed and to be constructed for **medical** and other applications (Uesaka, Ogino(Univ.Tokyo)).
2. **The higher harmonics** are being measured by using a strong permanent focusing magnet and so on (Yakimenko(BNL-ATF), Lim(LLNL)).
3. **Collective effects for the interaction of longer laser and lower energy-electrons** have been proposed and the simulation has been performed (Petrillo(Univ.Milan)).
3. A new scheme to use the **plasma channel guided electron beam** is proposed (Yoder(Manhattan College)).

# FEL and RF Photoinjectors

## 1. FEL

Gerald Andonian

“Observation of Ultra-wide Bandwidth SASE FEL”

Takahiro Watanabe

“Numerical simulation and experimental demonstration of seeded FEL at BNL-NSLS”

Kwang-Je Kim

“Quantum Effects in Gain and Start-up of Free Electron Lasers—Wigner Function Approach”

William Graves

“Longitudinal aspects of an ellipsoidal electron distribution and its effects on seeded FEL performance”

## 2. Application of RF Photoinjectors to Radiation Chemistry

Akira Sakumi

“Review of RF photoinjectors for radiation chemistry in the world”

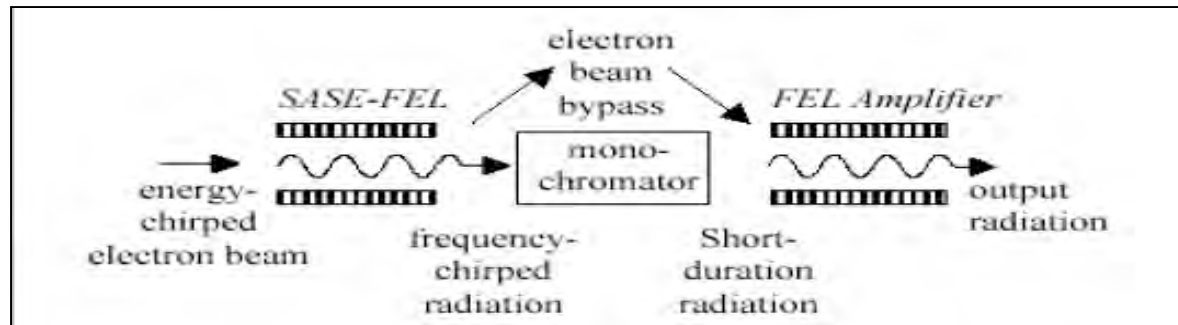
# Observation of Ultra-Wide Bandwidth SASE FEL

Gerard Andonian  
Particle Beam Physics Laboratory  
University of California Los Angeles

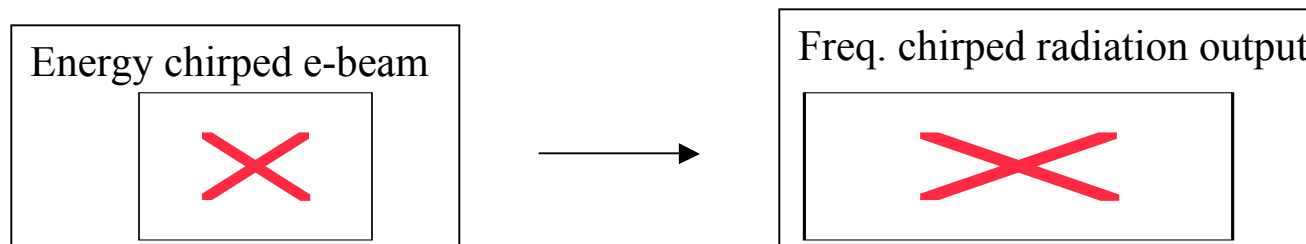
The Physics and Applications of High Brightness Electron Beams  
Erice, Sicily,  
October 9-14, 2005



# Motivation

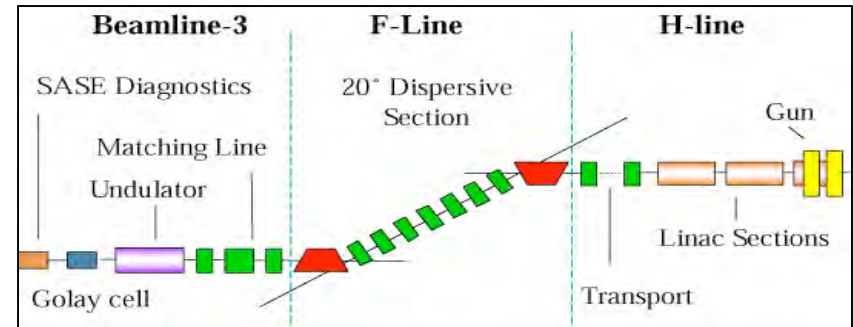


- Proposed Scheme for ultra short pulses
  - Energy chirped e-beam → FEL → freq. chirped radiation
- Explore Limits of SASE FEL with energy chirped e-beam
- Develop advanced beam manipulation & measurements



# Experiment Layout

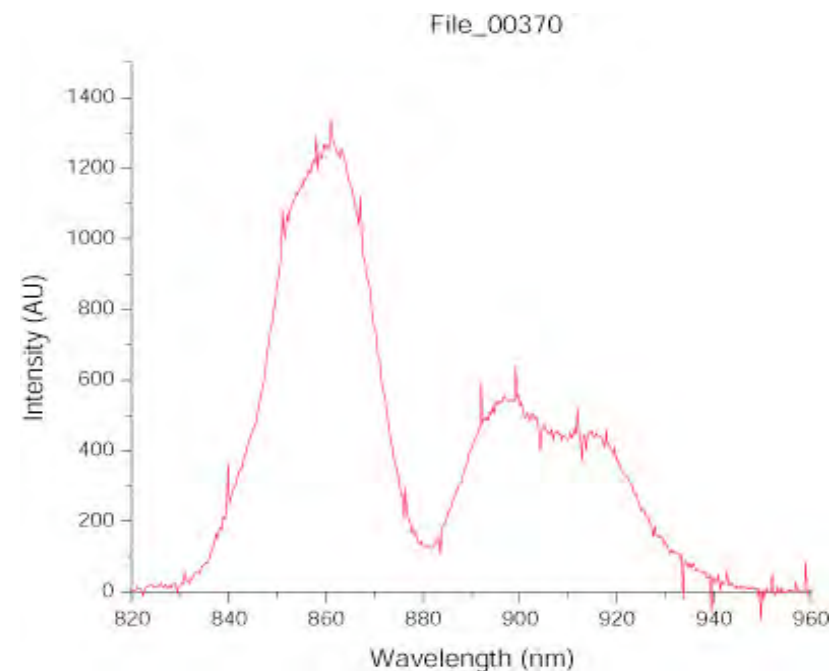
- Accelerator Test Facility (ATF) at BNL
  - Host for VISA I & II
  - 70 MeV beam
  - 28 m beam transport
    - 20 deg bend (F-line)
- Undulator
  - 4 x 1m sections
  - FODO lattice superimposed (25 cm period)
    - strong focusing
  - External steering coils (8)
  - Intra-undulator diagnostics
    - 50 cm apart
    - double-sided silicon
    - SASE FEL
    - e-beam (OTR)



VISA Undulator Parameters	
Undulator type	Planar (NdFeB)
Number of periods ( $N_u$ )	220
Peak field ( $B_{pk}$ )	.75 T
Undulator Period ( $\lambda_u$ )	1.8 cm
Gap (g)	6 mm
Undulator Parameter (K)	1.26

# VISA IB: Experiment

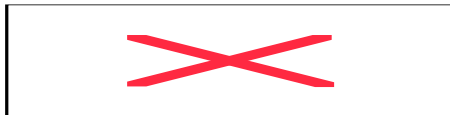
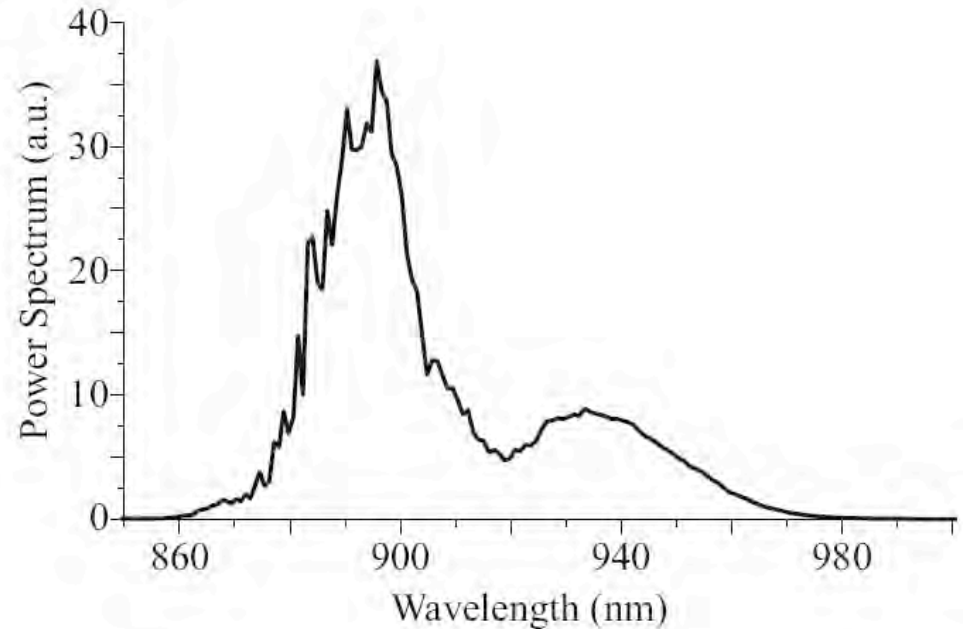
- High gain FEL
  - Chirped beam amplification
  - SASE energy  $\sim 2 \mu\text{J}$
  - close to saturation
- Up to 15% bandwidth observed
- Very reproducible and unusually stable
  - insensitive to RF drifts and phase jitter
- Characteristic double-spike structure



Wavelength Spectrum of FEL at VISA measured with Ocean Optics USB2000 Spectrometer.

# VISA IB: Analysis

- Start-to-End
  - Experimental Spectrum features reproduced
  - Angles Important
    - Off-axis Doppler Shift



FEL output Spectrum reproduced by  
Genesis (~10% bandwidth)

# Conclusions

- VISA yields rich data sets
  - VISA I, VISA IB
    - Observed ultra wide bandwidth
    - High gain chirped beam FEL
    - Further studies on hollow modes
  - Confidence in Start-to-end suite
- Develop new diagnostics
- Seeded amplifier runs & data forthcoming

# Numerical simulation and experimental demonstration of seeded FEL at BNL-NSLS

T. Watanabe, X.J. Wang, D. Liu, J.B. Murphy, J. Rose, T. Shaftan and L.H. Liu,  
BNL, USA  
P. Sprangle, NRL, USA  
S. Reiche, UCLA, USA

## Outline

- Directed energy application of FEL
- Numerical simulation of MW amplifier
- Experimental demonstration of seeded FEL

# Directed energy application of FEL

## Key issues

Megawatt ave. power

Compact

No optical damage

## Design of a Compact, Optically Guided, Pinched, Megawatt Class Free-Electron Laser

Phillip Sprangle, *Fellow, IEEE*, Bahman Hafizi, *Member, IEEE*, and Joseph R. Peñano

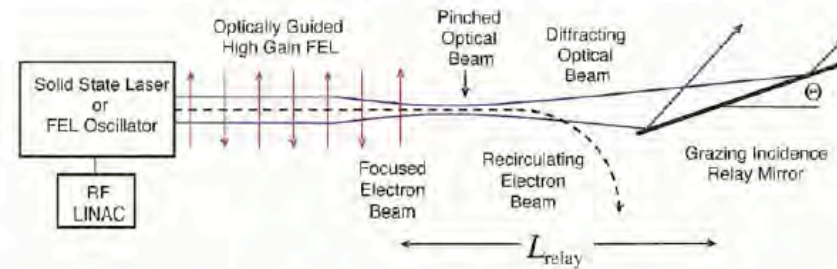
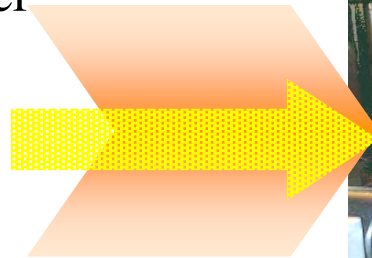


Fig. 1. Schematic of high-gain FEL amplifier with a grazing relay mirror. The input signal can be obtained from a solid-state laser or FEL oscillator. The radiation beam is optically guided in the wiggler and optically pinched at the exit. The pinched optical beam has a shortened Rayleigh range and undergoes rapid diffraction upon exiting the wiggler. Employing a grazing incidence configuration, the resultant footprint on the relay mirror can be made sufficiently large to avoid damage.

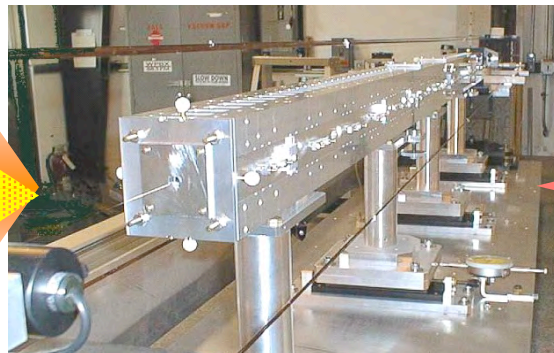
## This work

seed laser

e-beam  
65 MeV

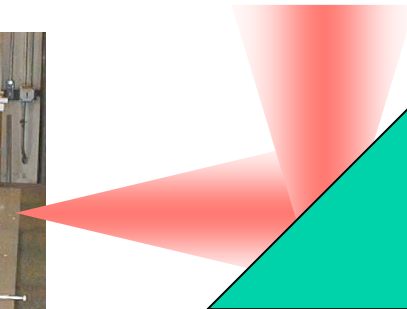


2-m VISA undulator  
w/ strong focusing



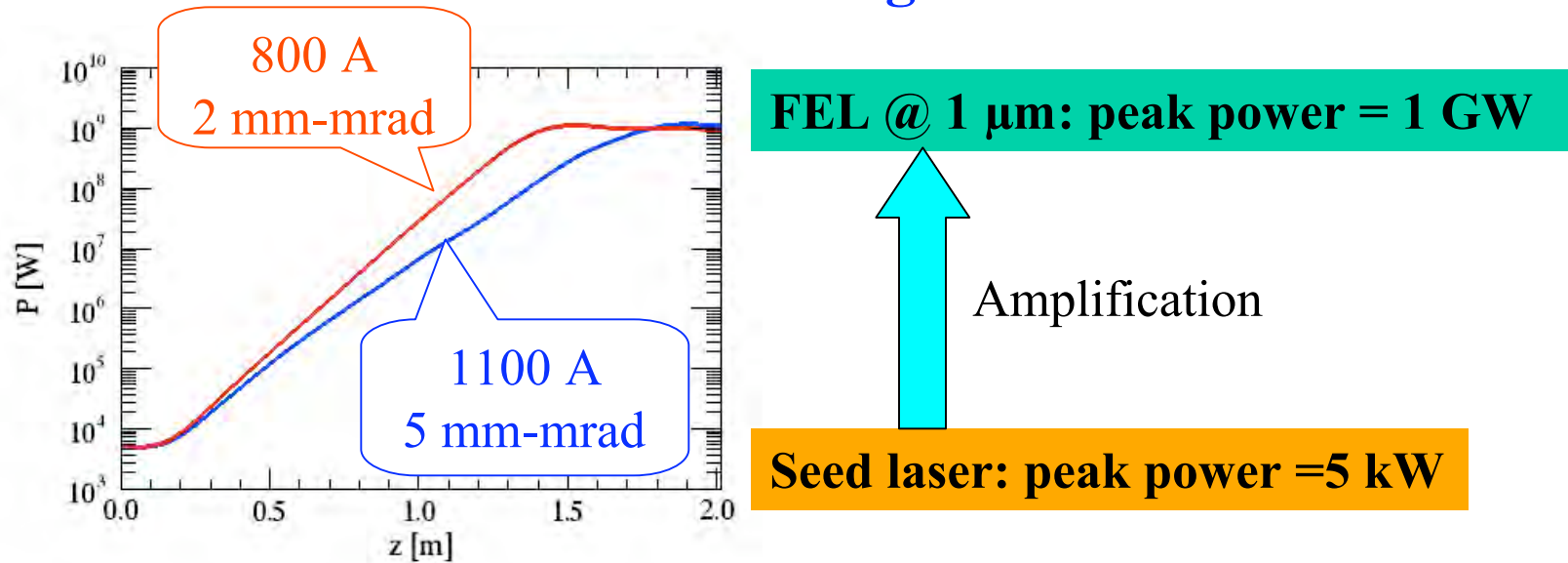
$K = 1.26$ ,  $\lambda_u = 1.8$  cm

1  $\mu$ m FEL

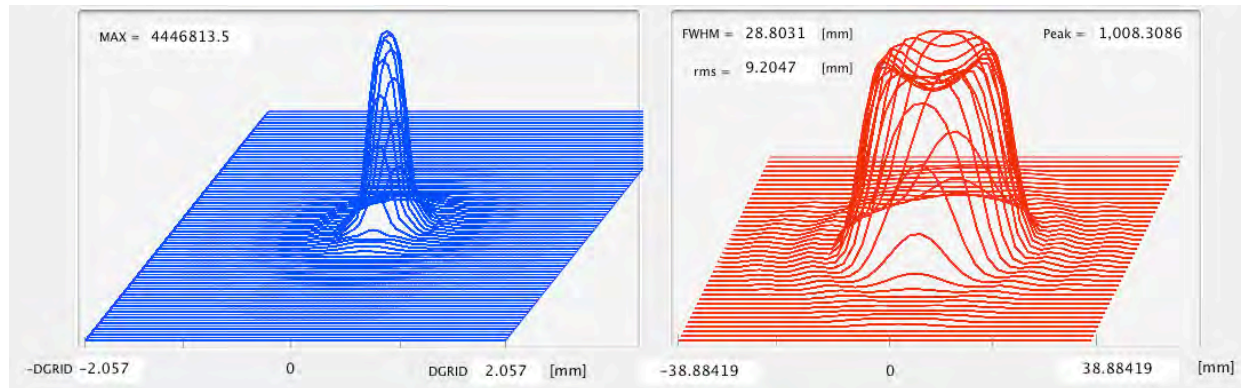


mirror

## Final design



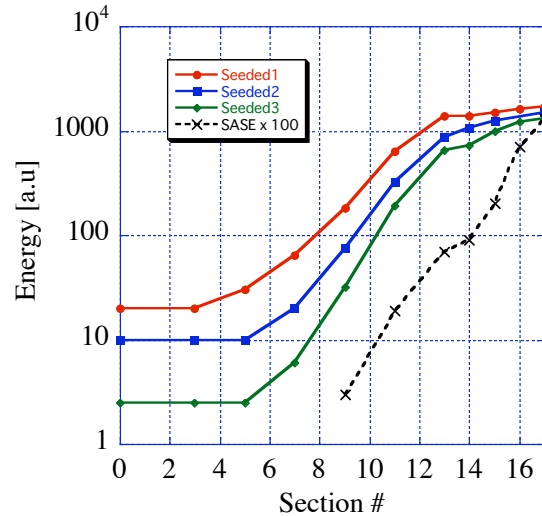
$$\text{Duty factor} = 1.4 \text{ [ps]} \times 700 \text{ [MHz]} = 0.1 \text{ [%]}$$



$$\frac{1.0 \text{ [MW]}}{\sqrt{2} \times \pi \times (1.5 \text{ [cm]})^2} \approx 100 \text{ [kW/cm}^2\text{]} \sim \text{damage threshold of mirror}$$



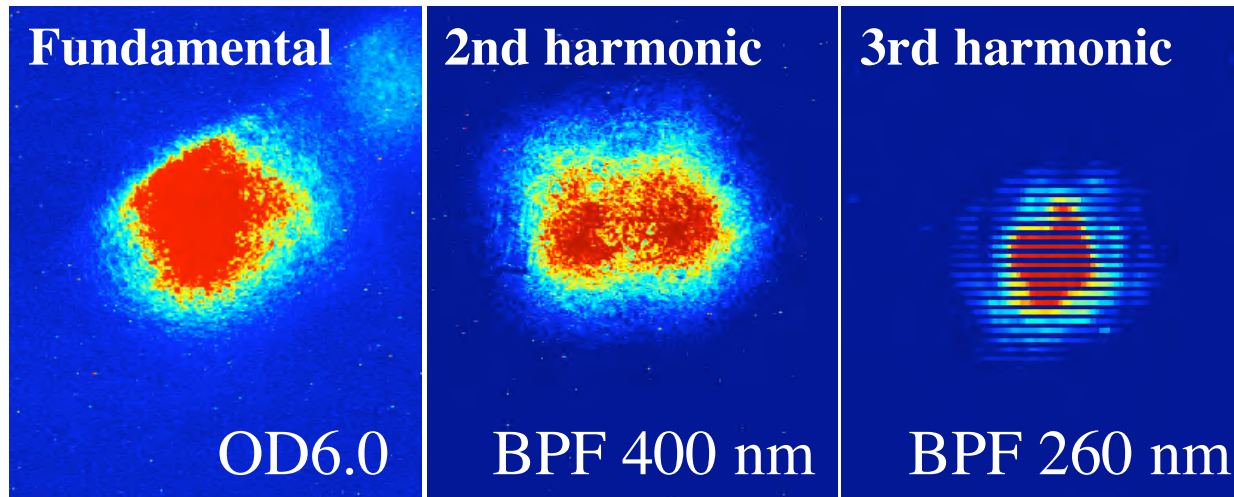
# Gain curves of seeded FEL



Gain length when radiation size is larger than e-beam size

$$L_G^{-1} = \frac{4\pi}{\lambda_u} \frac{3^{3/4}}{2} \sqrt{\frac{I}{\gamma I_A} \frac{K^2 [JJ]^2}{(1 + K^2/2)}}$$

## Spatial profiles of harmonics



\* Magnification of each image is different.

## Conclusion

MW class FEL was conceptually designed and seeded FEL in IR was experimentally demonstrated.

- SASE from 0.8 to 1.0  $\mu\text{m}$  observed.
- Gain curve of seeded FEL obtained.
- Spatial distributions of harmonics observed.
- Spectrum broadening due to laser chirp considered.
- Longitudinal distributions of harmonics measured.

## Future work

Repeat the experiment to verify

- Gain length v.s. input seed power
- Ratio of radiation size between each harmonic
- Longitudinal pulse duration at each harmonic

# **Longitudinal Studies of Ellipsoidal Bunches**

**William S. Graves**

**MIT**

**2005 Erice High Brightness Beams Workshop**

# Electron Beam Properties for Seeded FEL

## Beam needs depend on application:

- 1) Sufficient flat-top to allow harmonic cascade FEL using fresh bunch method (including timing jitter)
- 2) Long x-ray pulses generating meV bandwidth
- 3) Low energy spread allowing many harmonic cascade stages

Electron beam parameters do not need to be extreme, but we always want constant values of current and energy spread

• Ideal beam has 1 kA,  $\Delta E < 1$  keV, FWHM  $\sim 1$  ps

• Current variations  $\rightarrow$  FEL optical phase shifts due to gain variations

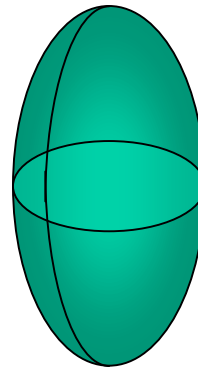
•  $dE/E$  variations  $\rightarrow$  inconsistent bunching  $\rightarrow$  FEL optical phase shifts

# Parmela Photoinjector Simulations

S-band injector

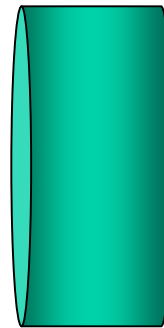
Compare ellipsoidal bunch with flattop.

RMS dimensions were set equal in each case



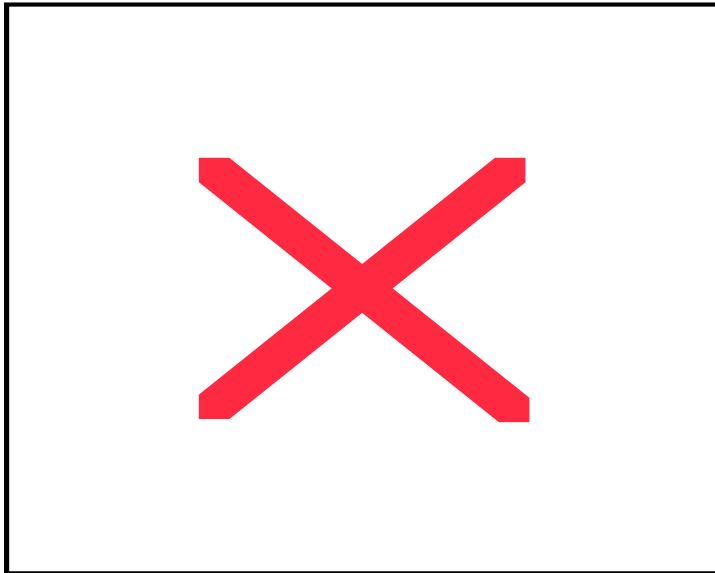
Ellipsoidal bunch

300 pC, ~1 mm radius,  
~5 ps full width

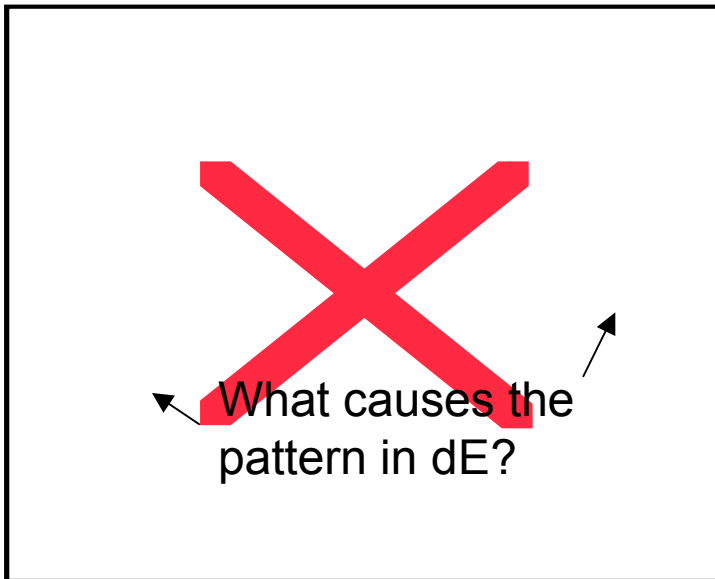
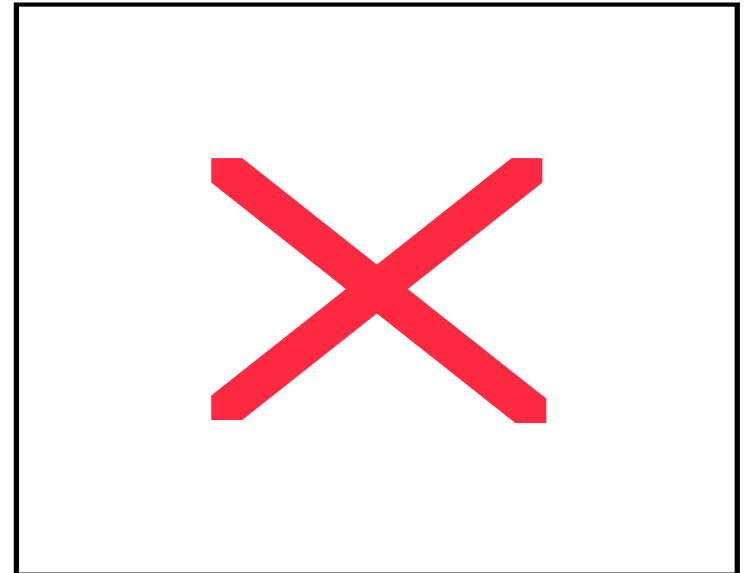


Flattop bunch

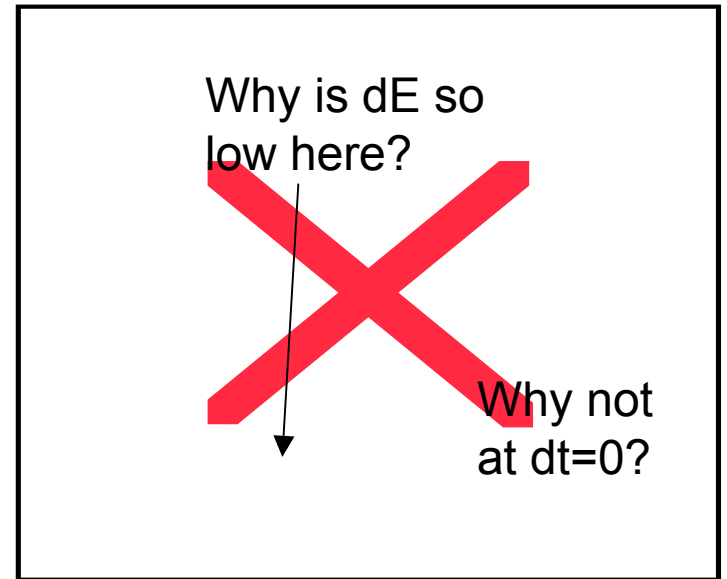
300 pC, ~1 mm radius,  
~5 ps full width



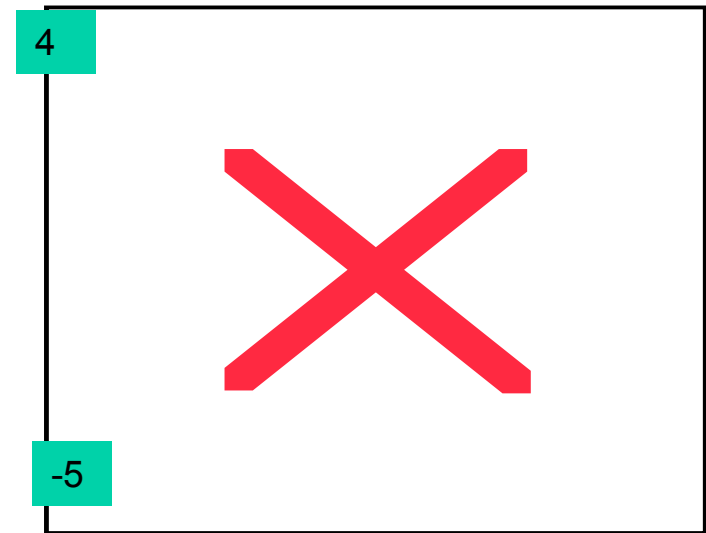
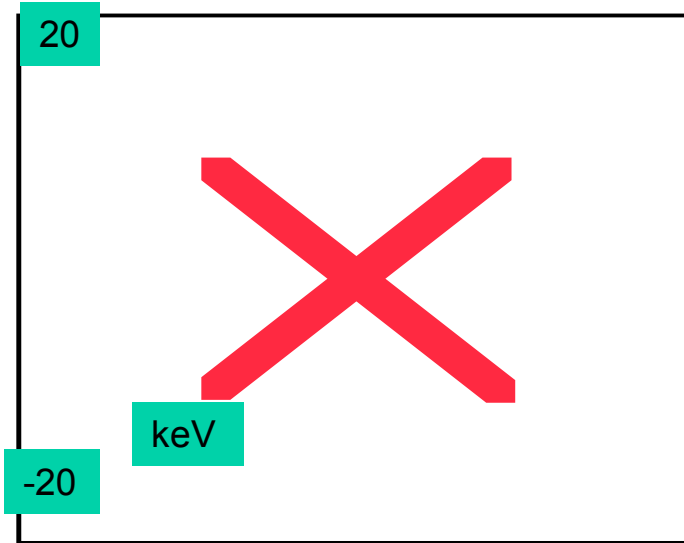
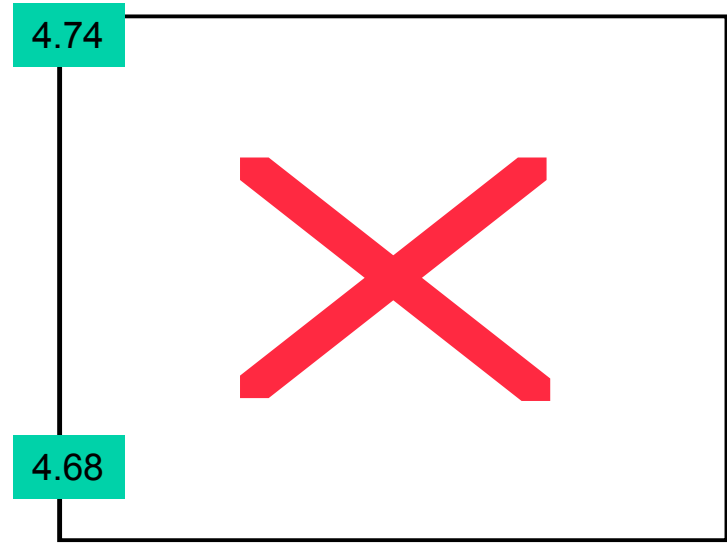
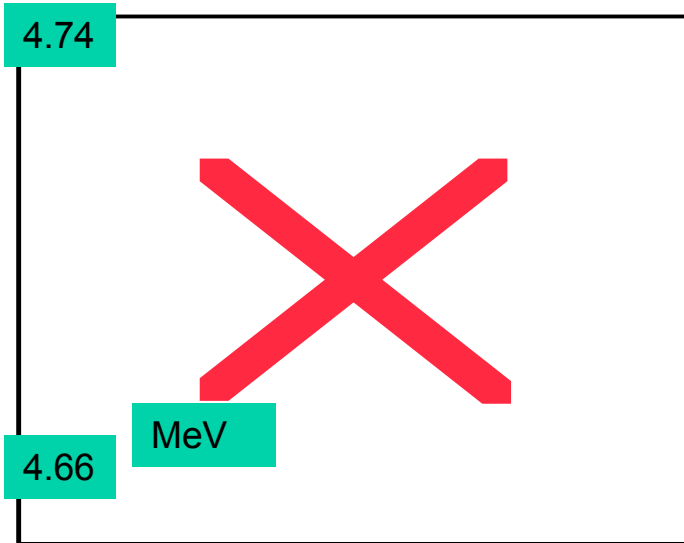
Current profiles for ellipsoid (left) and flattop (right).



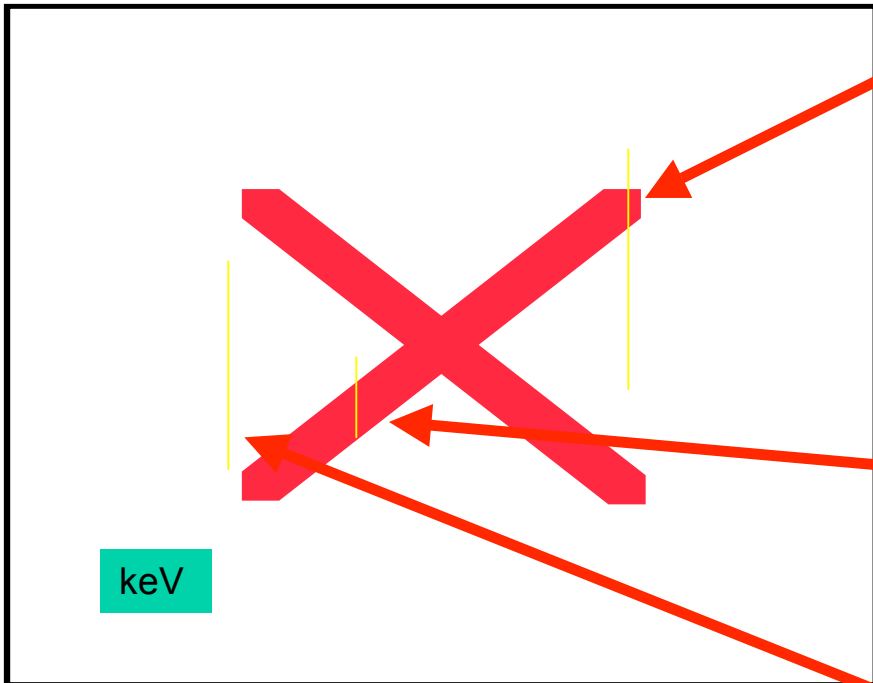
Energy spread for ellipsoid (left) and flattop (right).



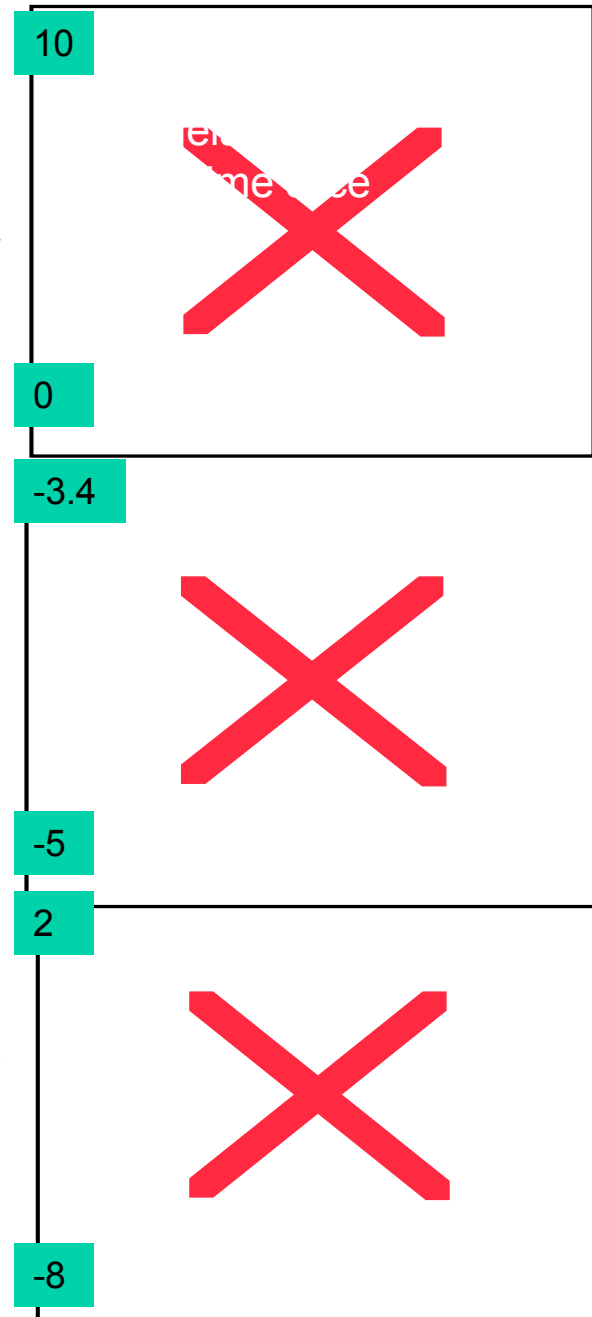
# Longitudinal Phase Space Density



Radial energy correlation reverses slope from head to tail for flattop bunch

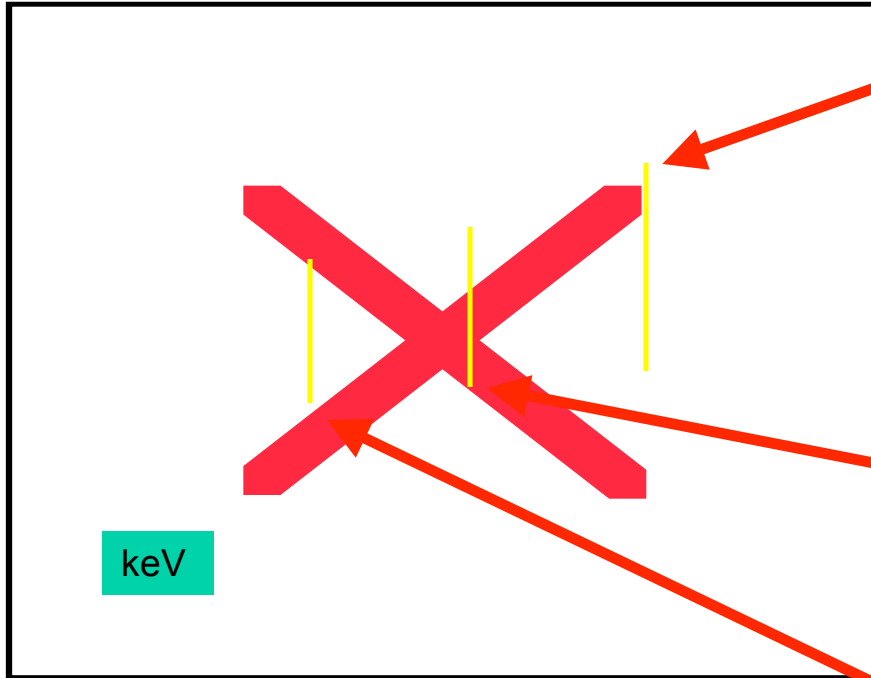


3 profiles show  $dE/E$  vs radius for the 3 short time slices above.

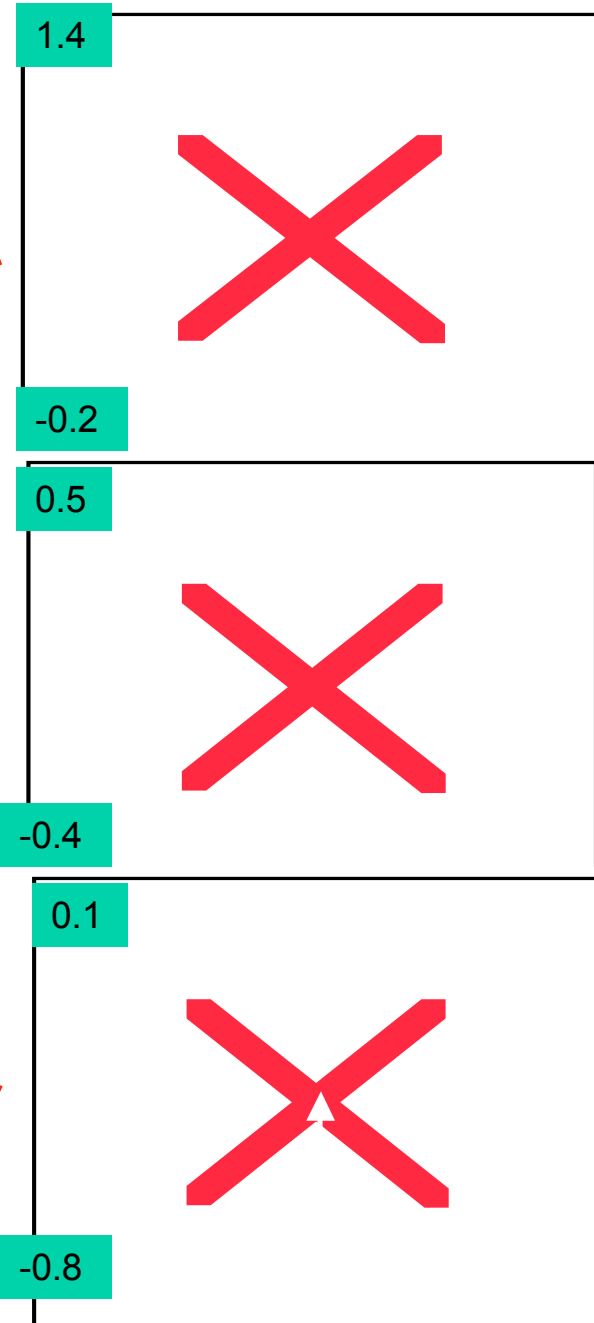




Lower charge (100 pC) balances RF correlation with space charge.  
Generates ultra-low  $dE/E$ .



3 profiles show  $dE/E$  vs radius for the 3 short time slices above.



## Summary

- Seeded FELs require constant current and energy spread for optimum performance.

- Ellipsoidal bunch distribution produces linear correlation of energy and time. Substantially improved over flat-top bunch.

- For thin time slices, all distributions show a strong correlation of energy with radius. Interesting new dynamics to study.

  - RMS  $dE/E \sim 100$  eV when radial correlation removed

  - Slope of correlation due to radial variation of RF field is opposite to that of space charge for ellipsoidal bunch

  - Slope of radial correlation for flattop bunch reverses sign from head to tail

# Quantum Effects in Gain and Start-up of Free-Electron Lasers — Wigner Function Approach

Zhirong Huang and Kwang-Je Kim

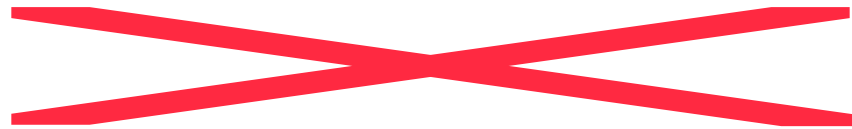
The Physics and Applications of High Brightness Electron  
Beams

Erice, Sicily

October 9-14, 2005

# Wigner Distribution Function

Given a wave-field, such as coherent EM field or quantum wave field as a function of spatial coordinate  $\theta$ , the W-function is a function of phase space coordinate  $(\theta, p)$



- $W$  is the closest object corresponding the classical phase space distribution. However, it is not a true distribution of particles since it can in general have negative values due to the fact that one cannot specify coordinate and conjugate momentum at the same time

- However  $W$  is useful because:

- It transforms as classical phase space distribution function

- integrals of  $W$  are positive and have a physical meaning :

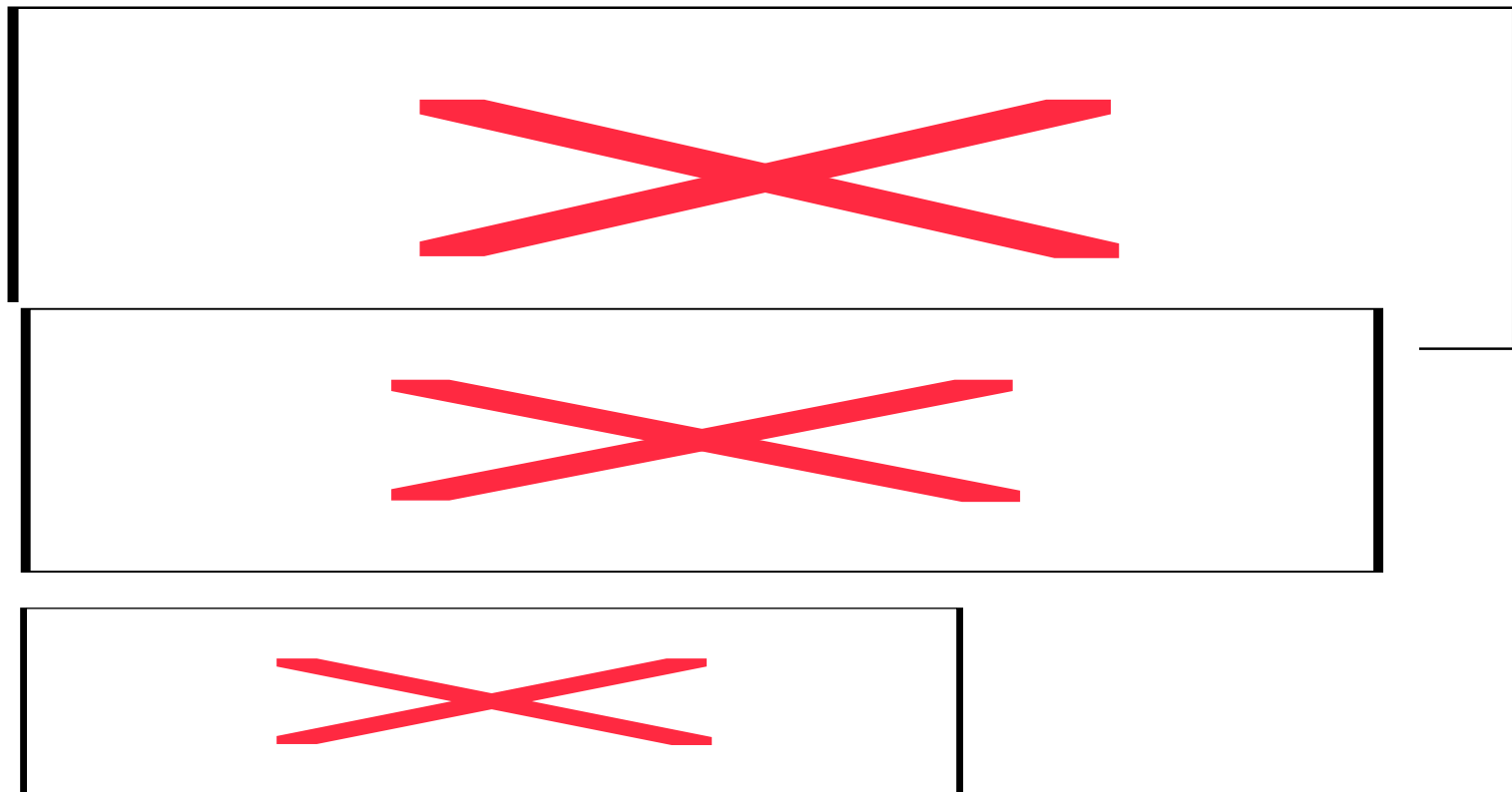
$$F(\theta, \tau) = \int dp W(\theta, p, \tau) = |\psi(\theta, \tau)|^2: \text{density}$$

$$V(p, \tau) = \int d\theta W(\theta, p, \tau) = \left| \int d\theta e^{ip\theta} f(\theta, \tau) \right|^2: \text{energy distribution}$$

# Solve Quantum Vlasov-Maxwell Equation for SASE

- Follow the classical derivation (KJK,1986)

Laplace transform  $\rightarrow$  solve in terms of initial values  $\rightarrow$  inverse Laplace Transform



is classical, smooth, average distribution

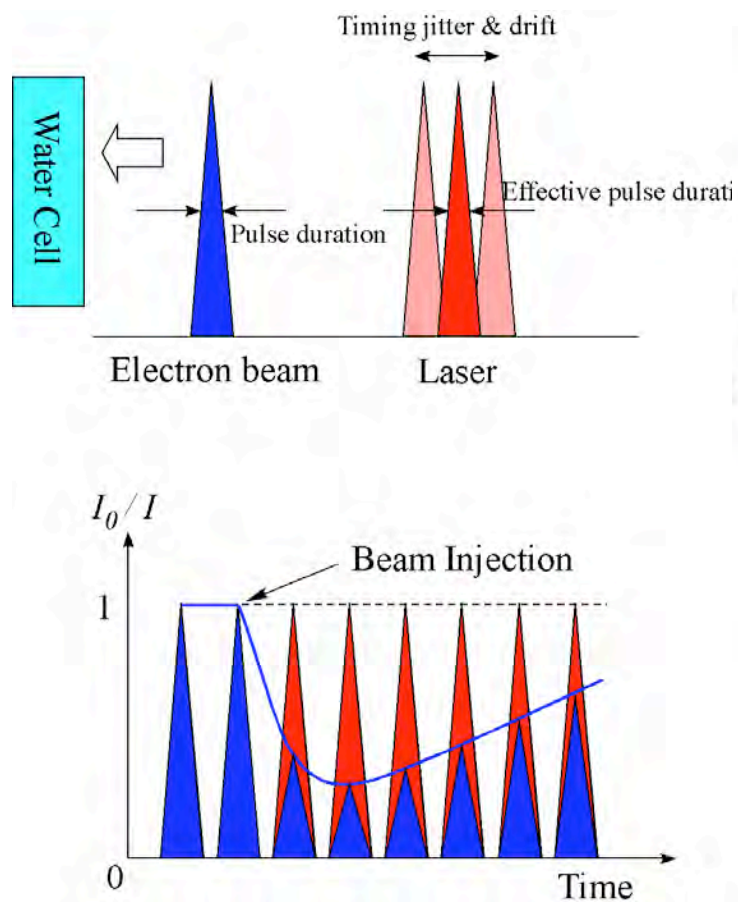
# Review of RF photoinjector for radiation chemistry

Univ. Tokyo

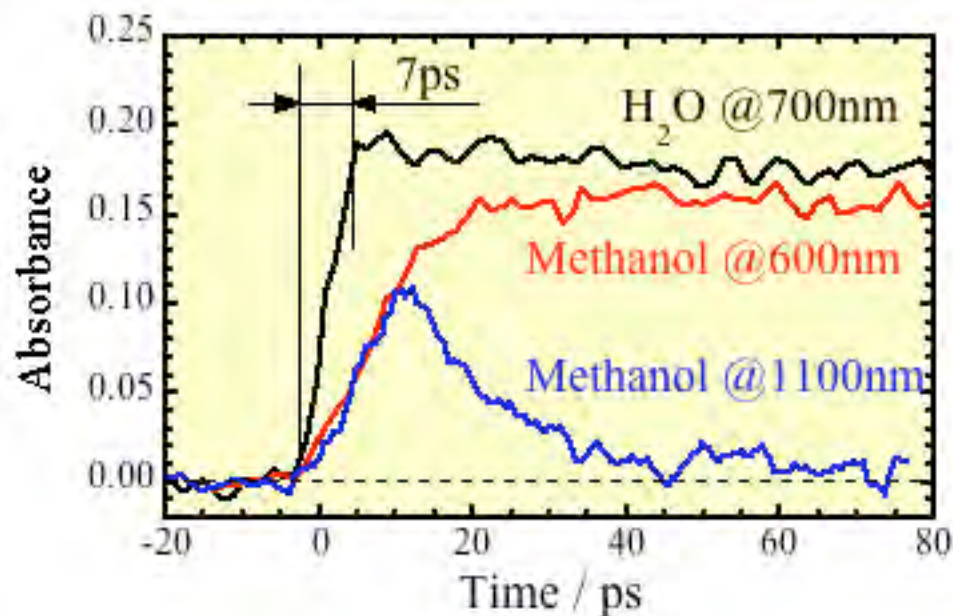
A. Sakumi, M. Uesaka, Y. Muroya, Y. Katsumura

# Radiation Chemistry

## Pulse radiolysis method



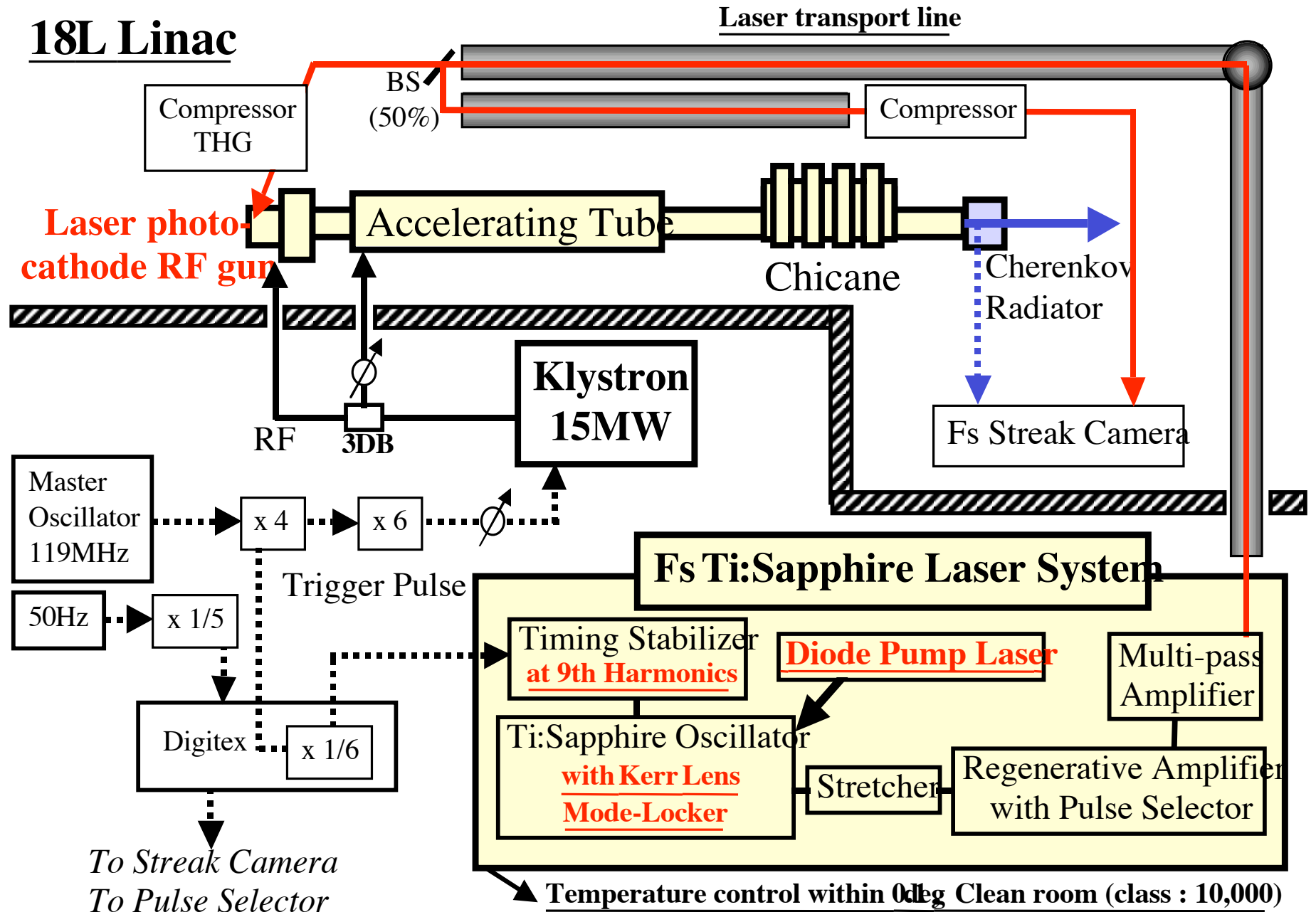
## Chemical reaction of water



NERS U. Tokyo Y. Muroya et al.,

# Precise Synchronization System at UTNS

Beam-Material Interaction  
www.utns.jp/~beam





ELYSE, Orsay



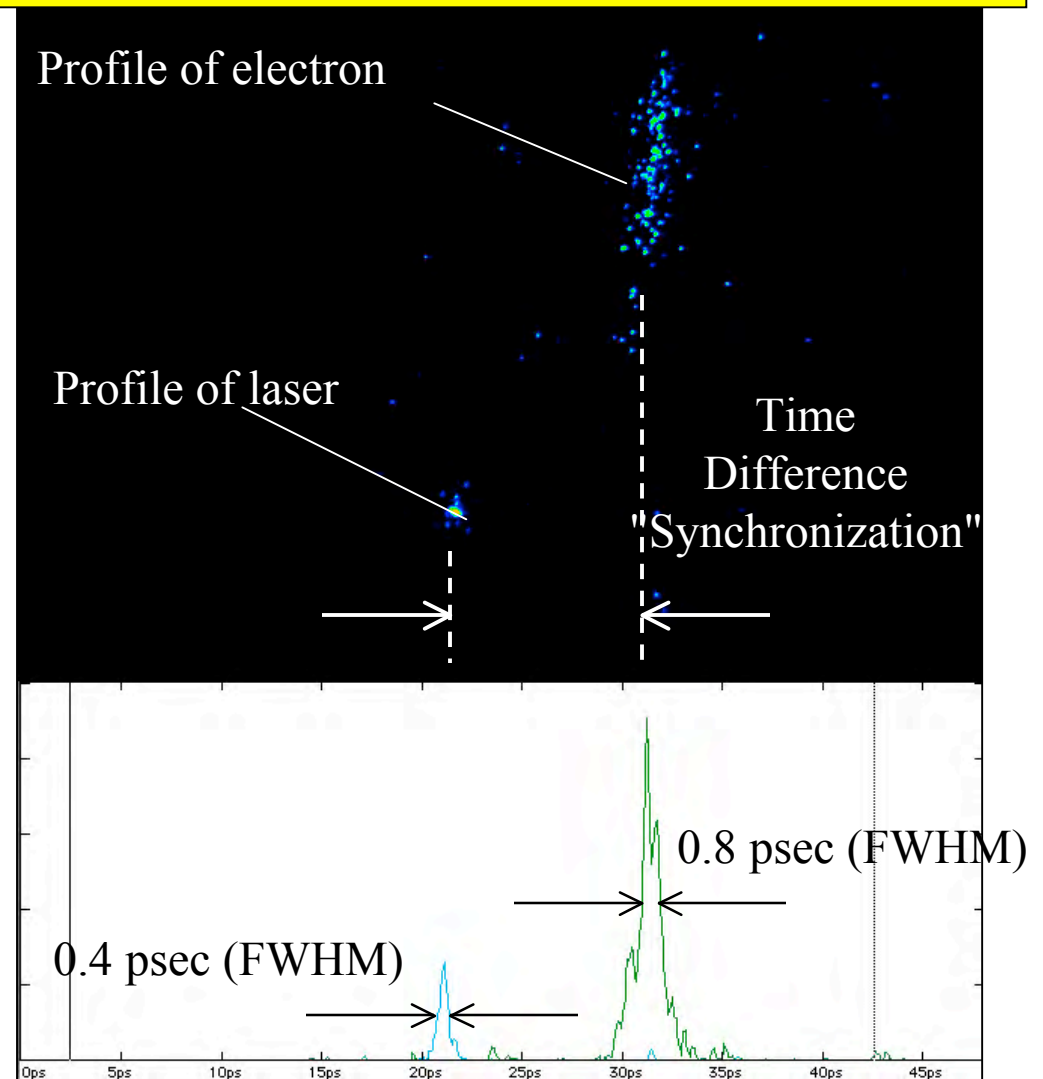
***ELYSE, Picosecond Pulse Radiolysis***

	Beam energy	Beam Current	Beam width	Beam size	Target path Length	Synchro - nization	Laser pulse width	Total time Resolutio n
U. Tokyo	4+18= 22MeV	2nC	1ps	3mm	1mm	<1ps(rms)	100fs(532nm-2600nm)OPA (400-1100nm) white light made by Ti:Sa	3ps(white light)
LEAF,BNL, USA	9MeV	2-8nC	$\geq 7$ ps		10mm(right water)	Pico-sec.	100fs(240-2600nm)OPA	>7ps(pulse-probe)
ELYSE, France	4 to 9 MeV	$\geq 1$ nC	$\leq 7$ ps	2-20mm				$\sim 7$ ps?
Waseda Univ.	4MeV	0.4-0.6nC						8ps
Osaka Univ.	38MeV	>0.2nC	<1ps				100fs	$\sim 5$ ps

# Requirement of stable synchronization

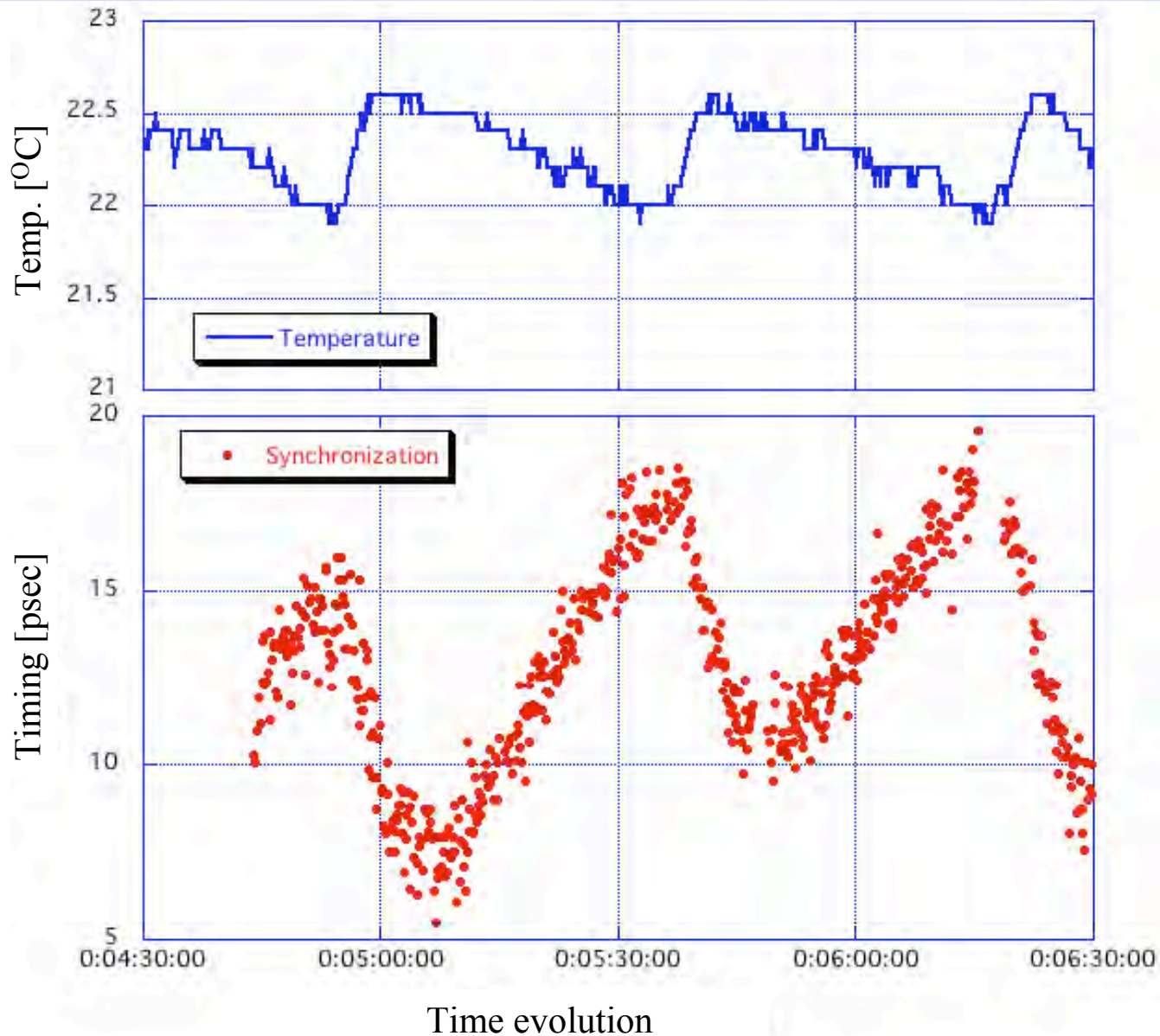
## Typical Femtosecond Streak Camera Image of Synchronization

- The S-band linac with Mg photocathode RF injector has been developed for radiation chemistry.
- The radiation chemistry experiment requires a time resolution in a range of sub-picosecond.
- The time resolution is defined by...  
*pulse duration of pump-beam, and probe-laser, synchronization between the beam and laser, and the beam intensity.*



The drift of the Laser-room temperature has much effort to Synchronization between laser and electron beam

---



# Summary of FEL and Photoinjector

1. **Ultra-wide bandwidth (15%) SASE FEL** has been observed at VISA, BNL-ATF ([Andonian\(UCLA\)](#)).
2. **Gain curve of seeded FEL and spatial profiles of harmonics** has been experimentally demonstrated and **1 GW system design** is shown. ([Watanabe\(BNL\)](#) ).
3. Longitudinal studies of ellipsoidal/flattop bunches were done to achieve low energy spread in the whole bunch. **Ellipsoidal bunch distribution produces linear correlation of energy and time.** Substantially improved over flat-top bunch. ([Graves\(MIT\)](#))
4. Discussion on the **QFEL** was done ([Kim\(ANL\)](#)).
5. **Photoinjectors for radiation chemistry** in the world are introduced, because they are the second-major users. **Suppression of the timing-jitter and long-term drift** between electron- and laser-pulses are discussed ([Sakumi\(Univ.Tokyo\)](#)).

# Plasma Wakefield Accelerations and Innovative Acceleration Schemes

## 1. PWA

Kenichi Kinoshita

“Application of Laser Plasma Cathode to Radiation Chemistry, All Thomson Scattering and Electron Microscopy”

## 2. Innovative Acceleration Schemes

Gil Travish

“Preliminary Results from the UCLA/SLAC Ultra-High Gradient Cerenkov Wakefield Accelerator Experiment”

Rodney Yoder

“Coupling Laser Power into a Slab-Symmetric Acceleration Structure”

S. Dabagov

“Channeling Projects at LNF”

Generation of energetic electrons from a laser plasma cathode  
and the future applications for pulse radiolysis,  
Thomson scattering X-ray generation,  
and electron microscopy

**K. Kinoshita, T. Hosokai, A. Zhidkov<sup>1</sup>, T. Ohkubo, A. Maekawa,  
K. Kobayashi and M. Uesaka**

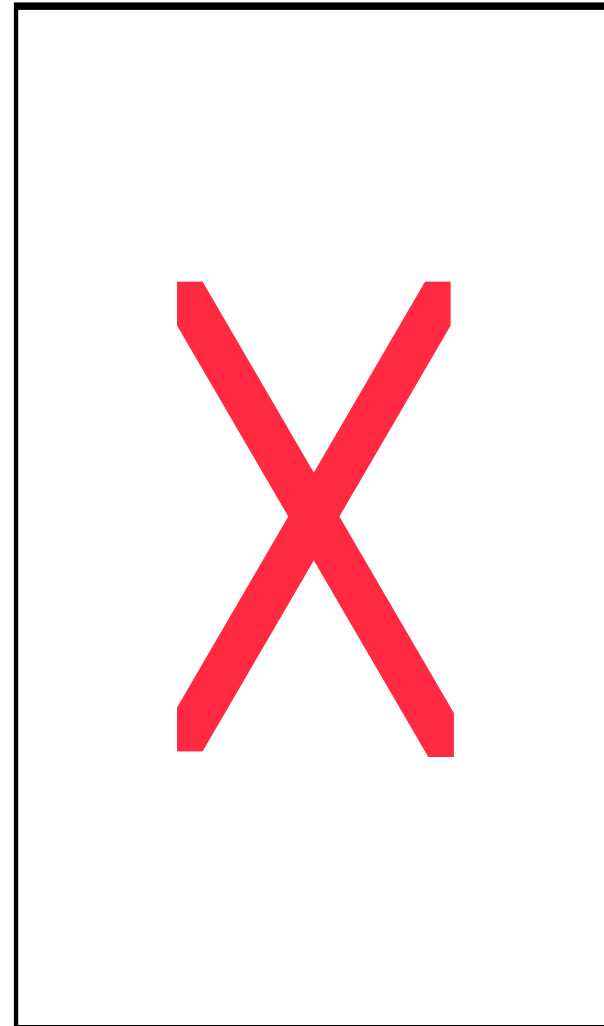
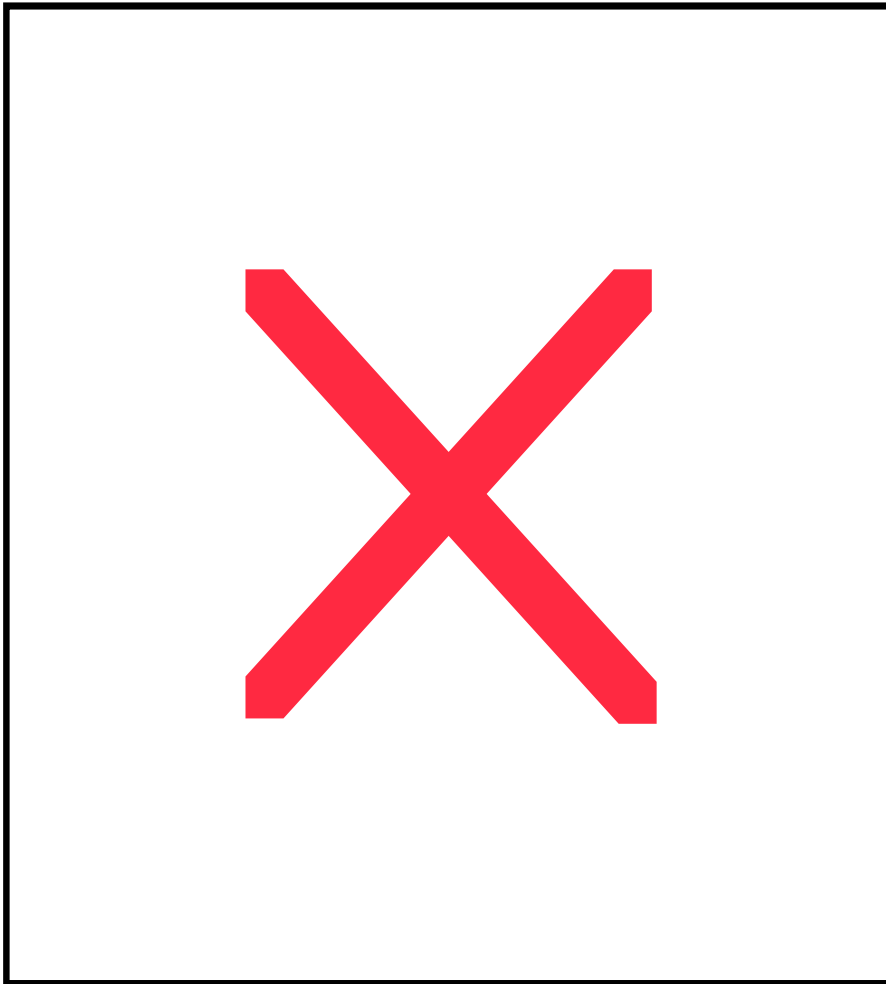
*Nuclear Professional School, School of Engineering, University of Tokyo*

*<sup>1</sup>National Institute of Radiological Sciences JAPAN*

# Mono energetic electron beam from laser plasma cathode

---

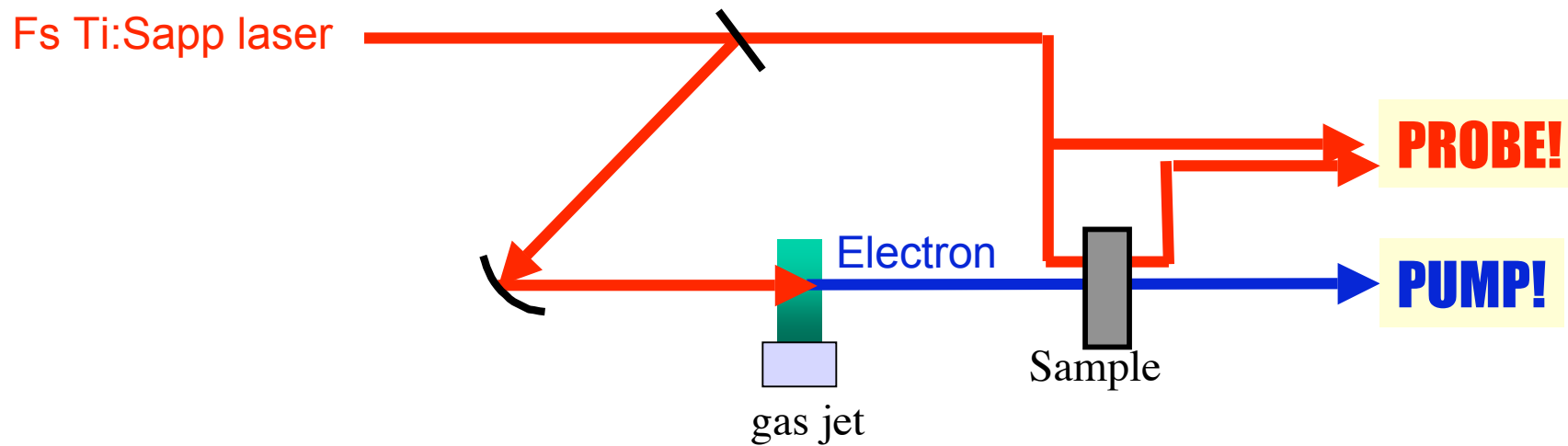
## Qasi mono energetic electron spectrum





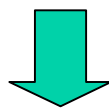
# Pulse radiolysis with laser plasma cathode

---



A laser pulse divided into electron generation pulse and probe pulse

- Jitter-free
- Femtosecond pulses

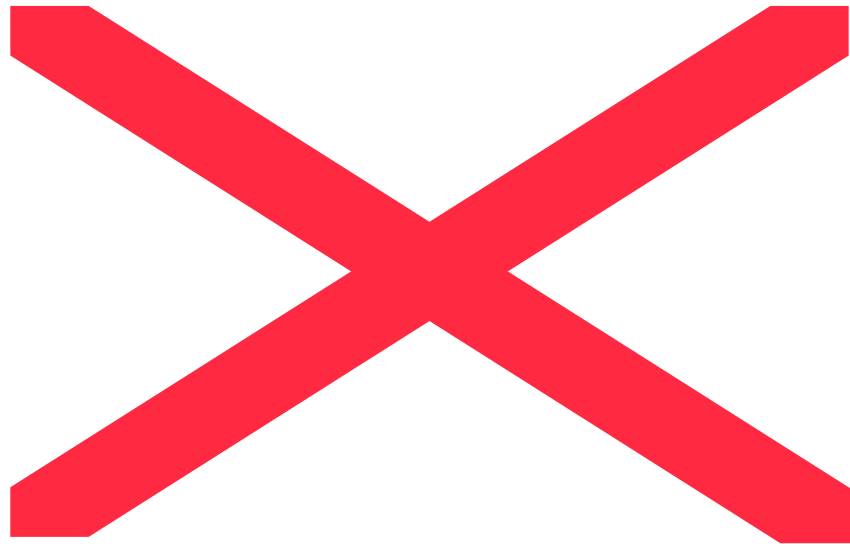


Femtosecond resolution!

Very simple setup!

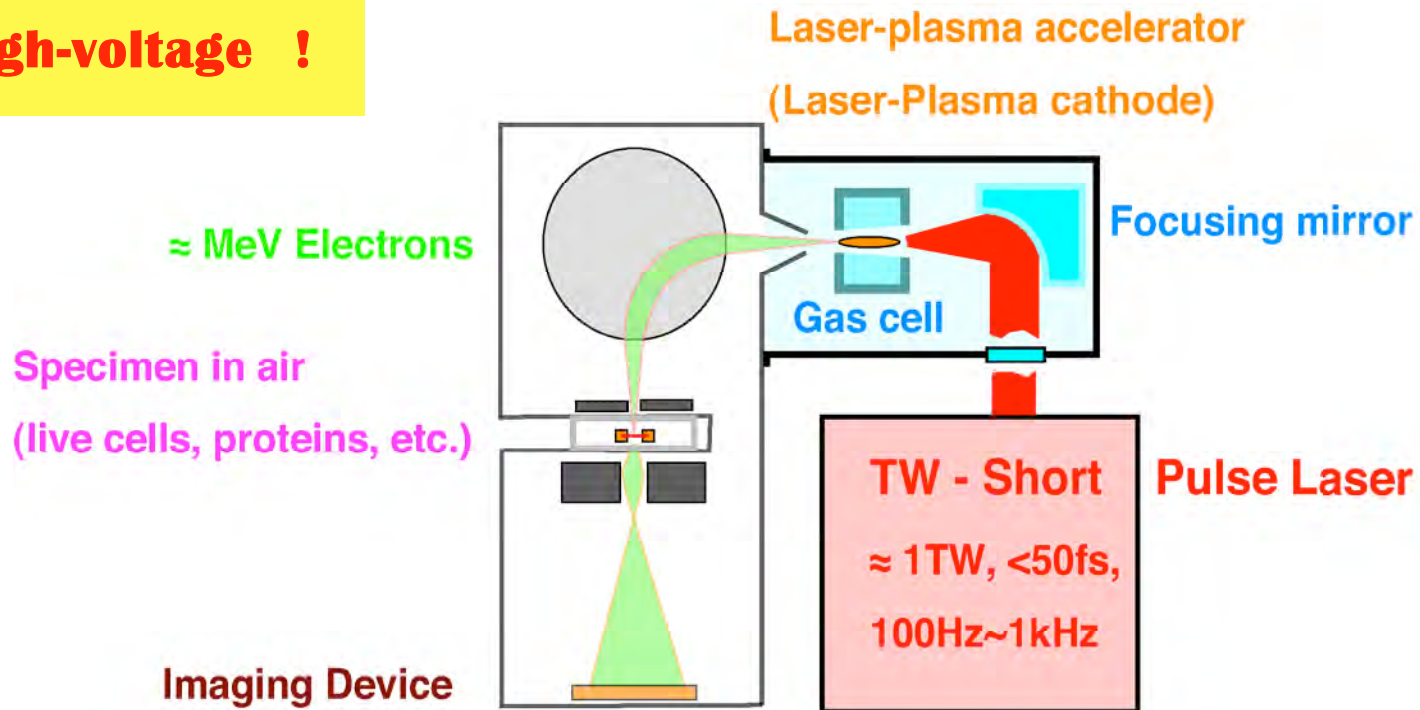
# Laser Thomson scattering with laser plasma cathode

---

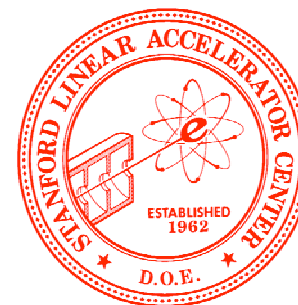


# A Strawman Design of Laser-driven Microscope

**No high-voltage !**



- Ultra-short pulse of  $\approx 10$ fs might be possible to accelerate electrons in the atmospheric pressure.
- Laser-plasma cathode technique will enable us to observe live specimen by the electron microscope.
- Pump-probe technique with fs-resolution will be possible.



## **Preliminary Results from the UCLA/SLAC Ultra-High Gradient Cerenkov Wakefield Accelerator Experiment**

M. C. Thompson<sup>†</sup>, H. Badakov, J. B. Rosenzweig, G. Travish\*  
UCLA Dept. of Physics and Astronomy

M. Hogan, R. Ischebeck, N. Kirby, R. Siemann, D. Walz  
Stanford Linear Accelerator Center

P. Muggli – University of Southern California

A. Scott – UCSB Dept. of Physics      R. Yoder - Manhattan College



\*Spokesman for the Collaboration at Erice

<sup>†</sup>Current Affiliation:  
Lawrence Livermore National Laboratory

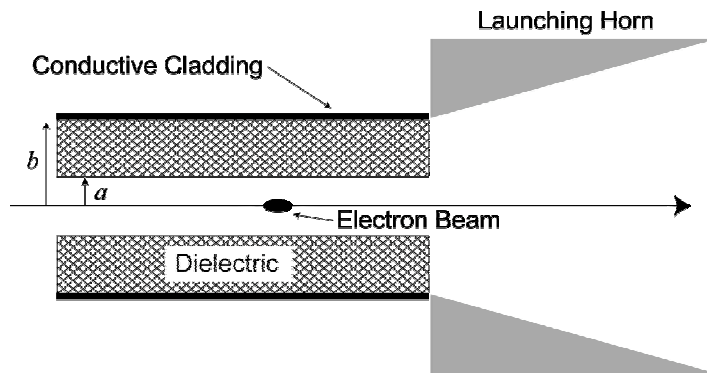


# High Frequency Dielectric Accelerators

Dielectric accelerating structures can be driven by many different mechanisms at frequencies from microwave to optical, but **electron driven structures operating at THz frequencies** have several advantages:

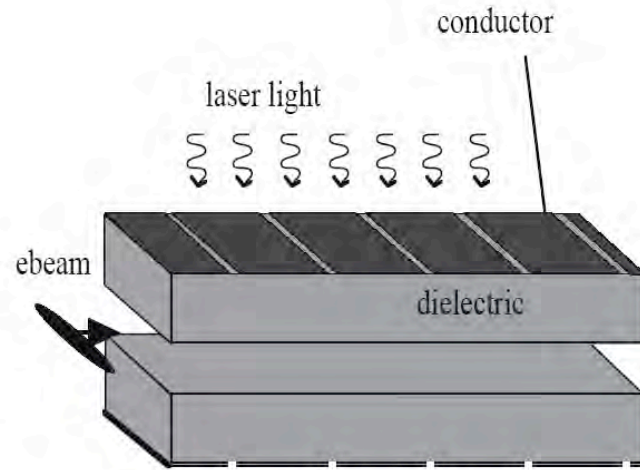
**High power THz range operation without external THz source.**

**Possible breakdown suppression due to relatively low drive beam field photon energies.**



Schematic of a Electron Beam Driven Dielectric Wake Accelerator.

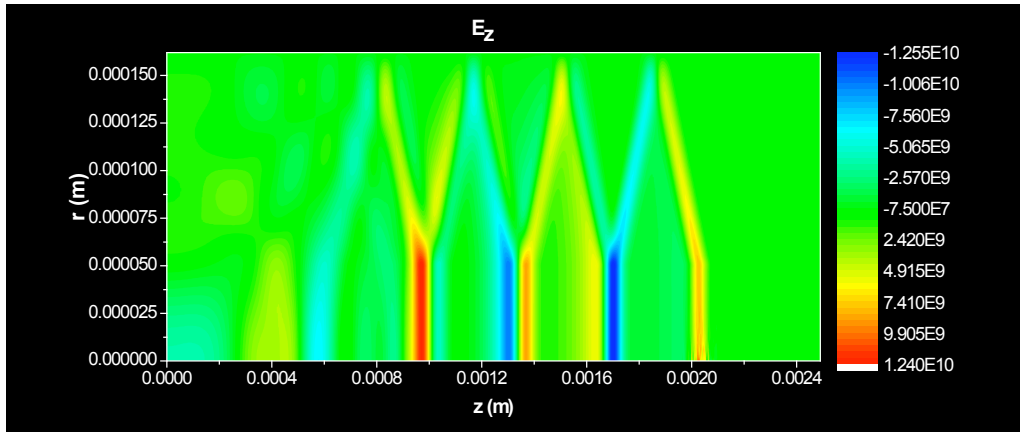
**Plasma accelerator class GV/m accelerating fields without the problem of ion collapse.**



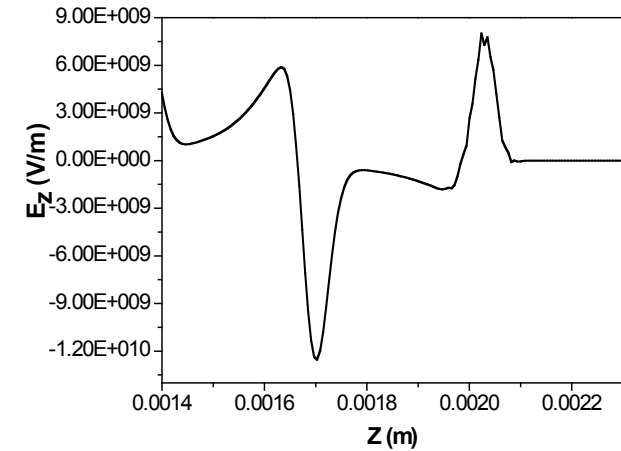
Courtesy R. Yoder

Schematic of a Laser Driven Dielectric Accelerator Structure.

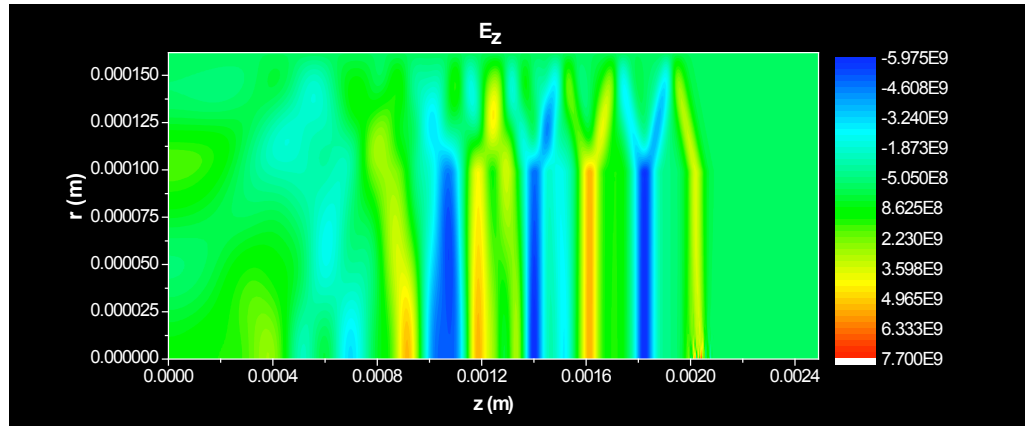
# OOPIC Simulations for $a_z = 20 \mu\text{m}$



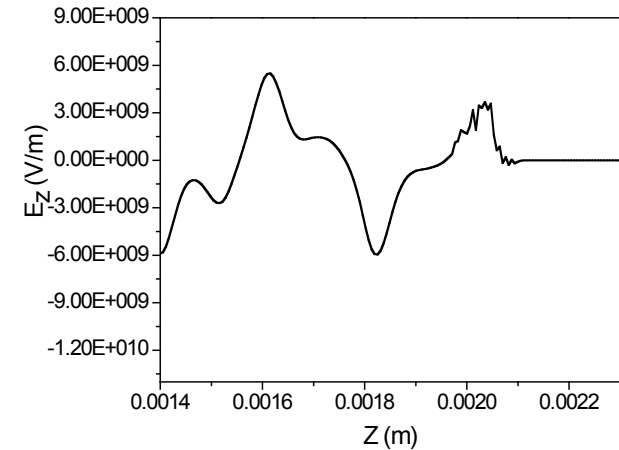
Contour plot showing  $E_z$  for  $a = 50 \mu\text{m}$



Line out of  $E_z$  at  $r = 10 \mu\text{m}$  with  $a = 50 \mu\text{m}$



Contour plot showing  $E_z$  for  $a = 100 \mu\text{m}$



Line out of  $E_z$  at  $r = 10 \mu\text{m}$  with  $a = 100 \mu\text{m}$

# Realizing the Experiment

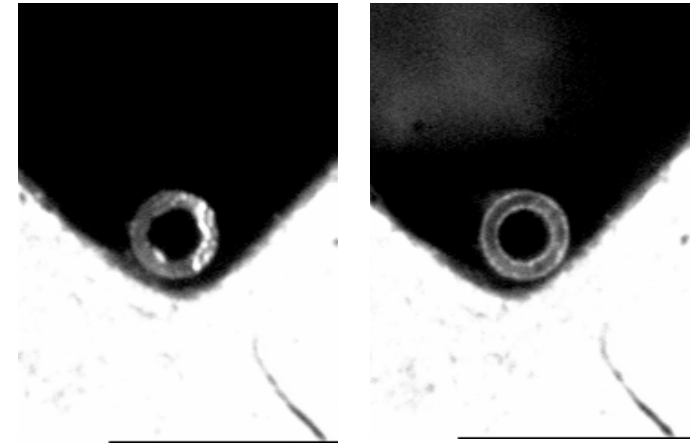
---

**Dielectric Tube Samples** for this experiment were modified from off the shelf synthetic fused silica capillary tubing ( $n \approx 3$ ), which we were able to purchase in 100 and 200  $\mu\text{m}$  ID sizes and coat on the outside with aluminum.

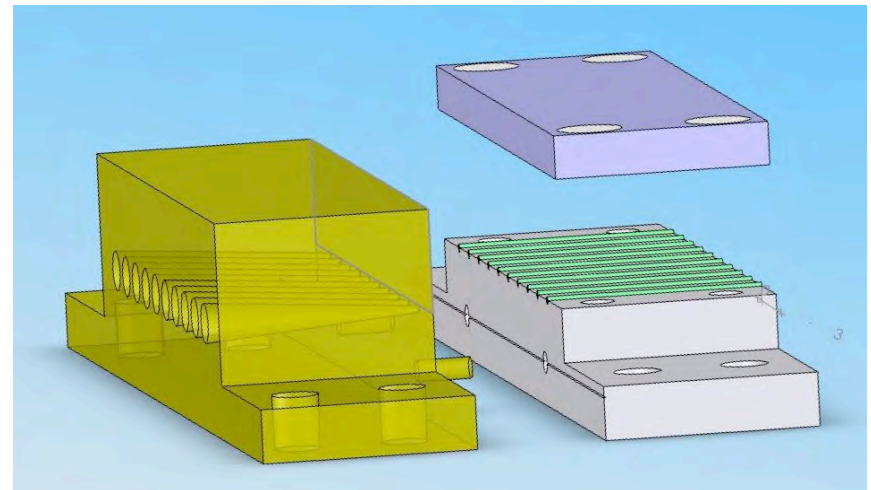
**Mounting Blocks** are used to hold 10 dielectric tube samples for the experiment. The mounting block are placed on motorized optics mounts and stages so the various samples can be placed onto the beam orbit.

**High-Resolution Video Cameras** look for optical emissions associated with the breakdown events. We also examine the dielectric tubes after the run to analyze structure damage from breakdown.

**Launching Horns**, similar to those used in microwave antennas, will boost amount of CCR delivered to the pyroelectric detectors.



Fiber viewed end on with a microscope. Unpolished at left and polished at right.



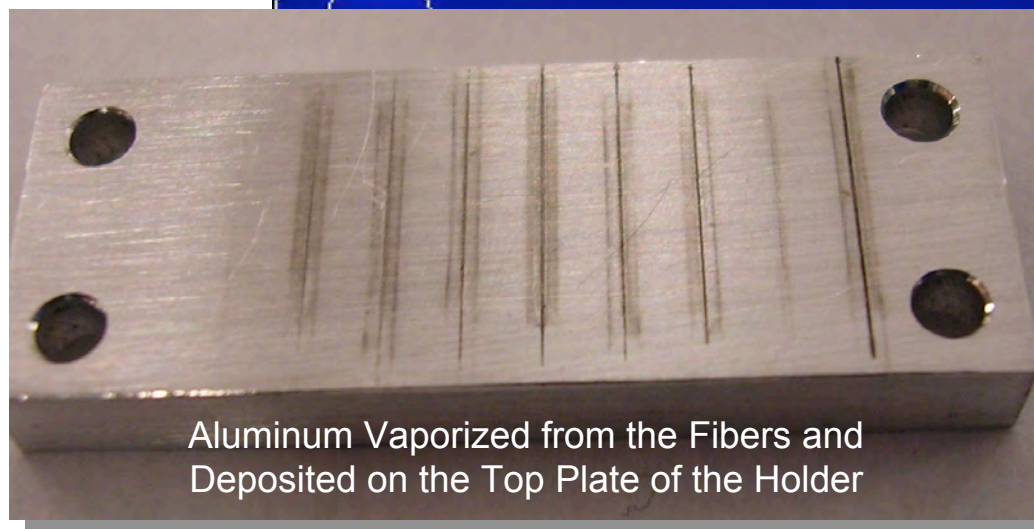
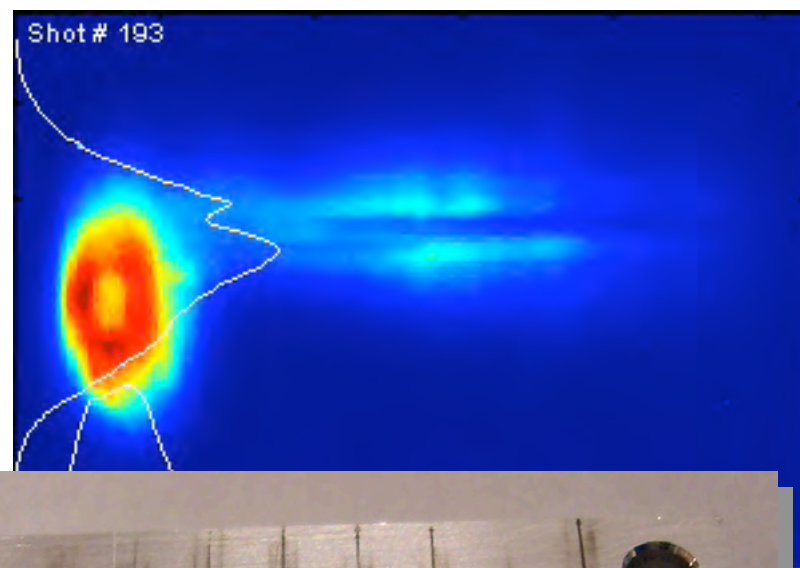
CAD rendering of the capillary tube mounting block with detachable launching horns.

# Phase One of the Experiment

The first run of the experiment occurred in Aug 2005. The objective of the run was to examine breakdown thresholds. Direct Measurements of CCR will be attempted in the next run.

## Major Observations:

- A sharp increase in visible emission from the capillaries near the mid-range of beam current, probably indicating breakdown.
- Principle form of damage to the dielectric wake structures appear to be vaporization of the aluminum cladding. The fused silica appeared substantially intact.





# Breakdown Observations

Most of the observations were of 200  $\mu\text{m}$  ID fibers and the general impression is that the visible light output of the fibers jumped up sharply in the middle of the beam pulse length range. We theorize that the initiation of breakdown discharges are responsible for the increase.

### Visible Light Sources Below Threshold:

- Incoherent Cerenkov Radiation, Incoherent Transition Radiation, Scintillation

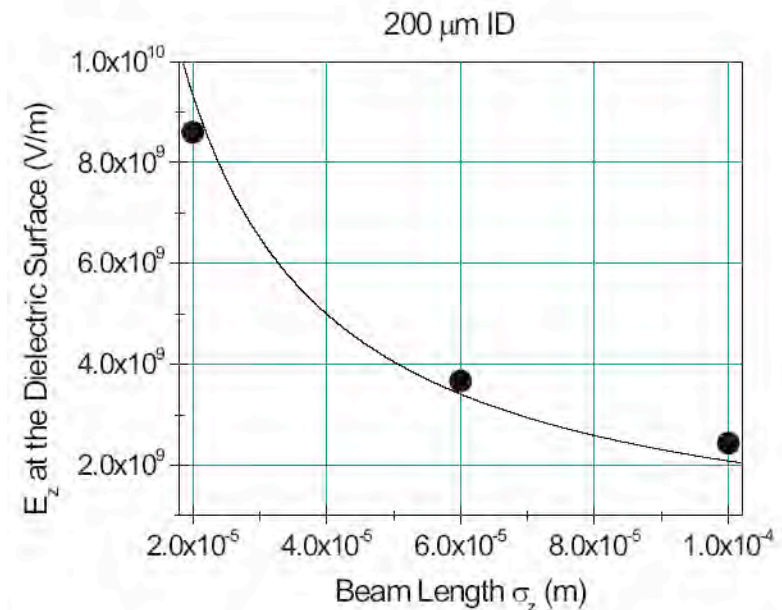
### Visible Light Sources Above Threshold:

- All of the above plus emissions from Plasma formed during breakdown events.

Breakdown fields implied by these preliminary observations should they be confirmed by further analysis:

- ~ 4 GV/m at the dielectric surface
- ~ 2 GV/m on axis accelerating field

*We are working to quantify these observations.*



# Conclusions

---

- The prospects for developing GV/m class dielectric accelerators look promising.
- It appears that fused silica holds up well under fields at the GV/m level.
- Resistive heating of the conductive cladding is a significant problem in this extreme environment.

## *Future Directions*

---

- Further data analysis on all aspects of the experiment should give more insight.
- Clearly the fiber cladding will need to be redesigned with the aim of reducing resistance and increasing thermal coupling.
- The next round of experiments will include measurements of the coherent Cerenkov radiation emitted from the fiber, which will give us more information about the field strengths within the fiber.

# Coupling Laser Power into a Slab-Symmetric Accelerator Structure

R. B. Yoder

*Manhattan College, New York*

J. B. Rosenzweig

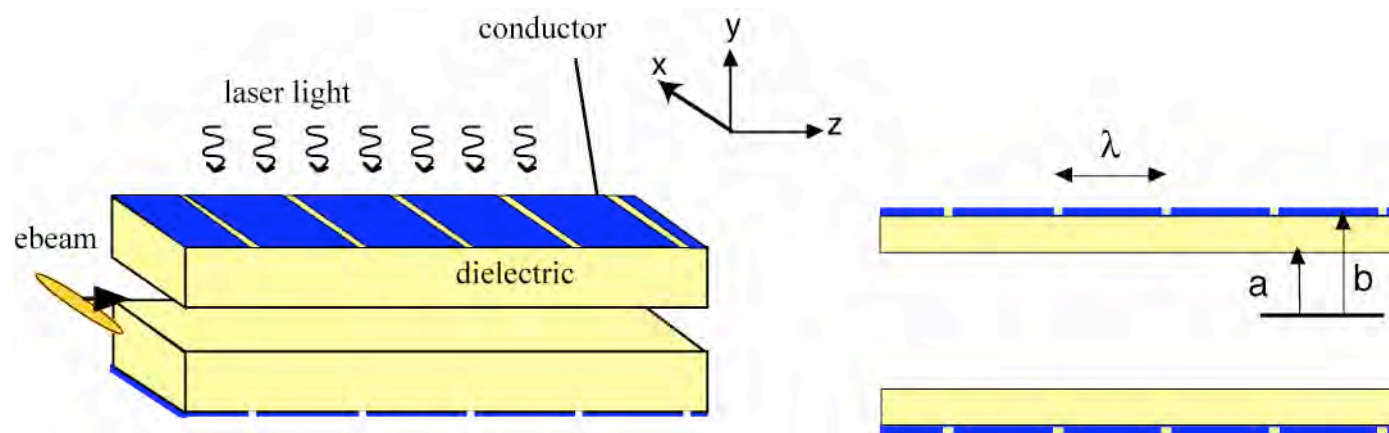
*UCLA Dept. of Physics and Astronomy*

ICFA Workshop on High-Brightness

Beams,

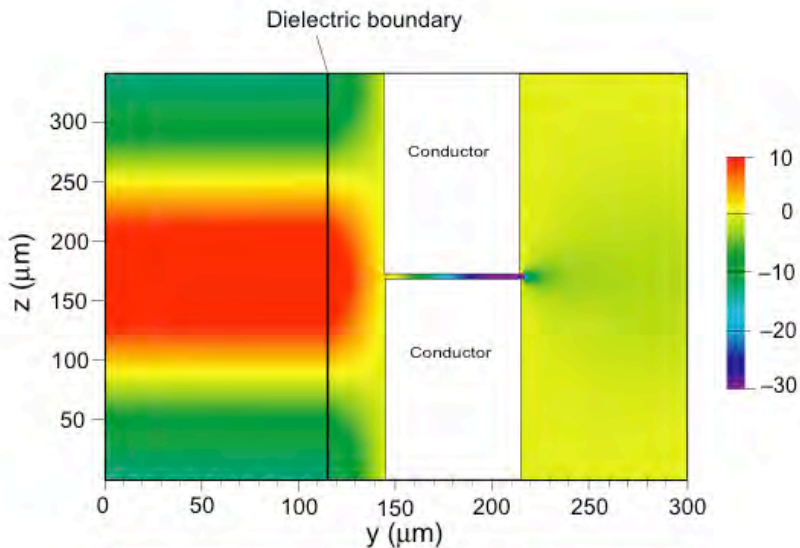
Erice, October 2005

# The Structure: cartoon



Typical dimensions:  $\lambda$  matches drive wavelength ( $10 \mu\text{m} - 340 \mu\text{m}$ )  
Length (in  $z$ )  $\sim$  width (in  $x$ )  $\sim$  laser spot size (a few cm)  
 $a, b$  are a fraction of  $\lambda$

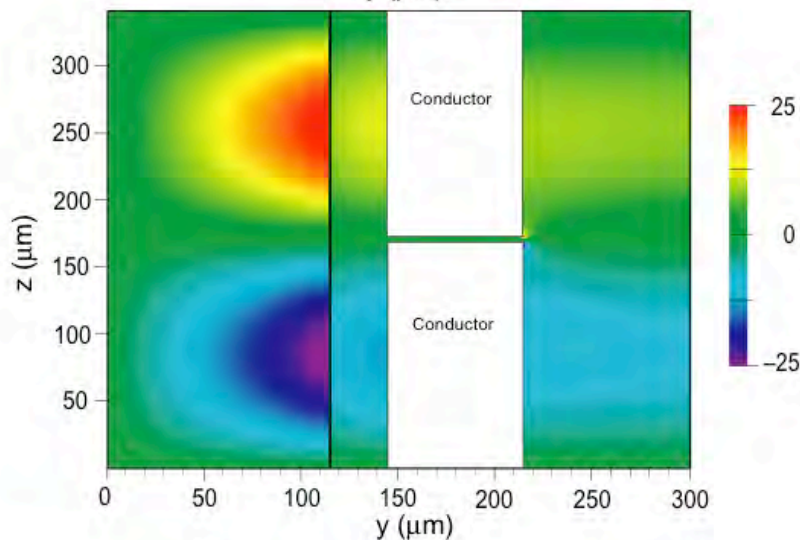
# 2D time-dependent simulation



340  $\mu\text{m}$  wavelength  
 $a = 115$   $\mu\text{m}$ ,  $b - a = 30$   $\mu\text{m}$   
quarter-wavelength slots  
slot width = 5  $\mu\text{m}$

Axial field:

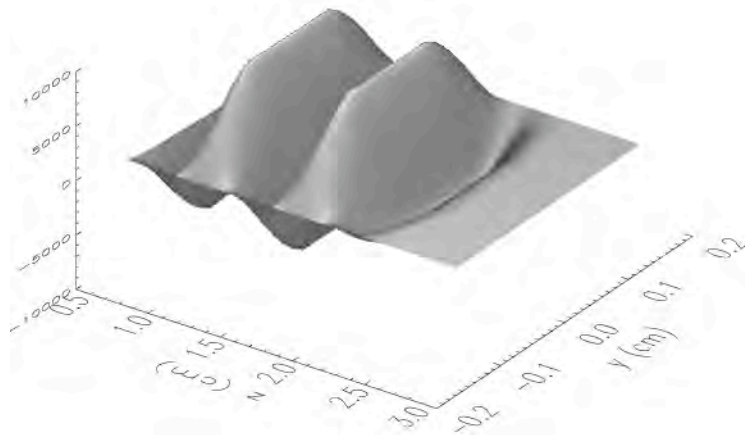
- flat wavefronts (no perturbation)
- large field in slot (3x peak)



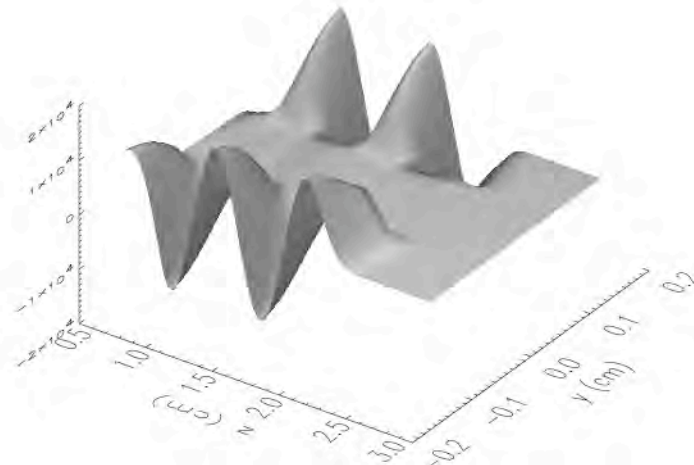
Transverse field:

- zero at  $y=0$
- zero at peak acceleration

# Wakefields: Without slots

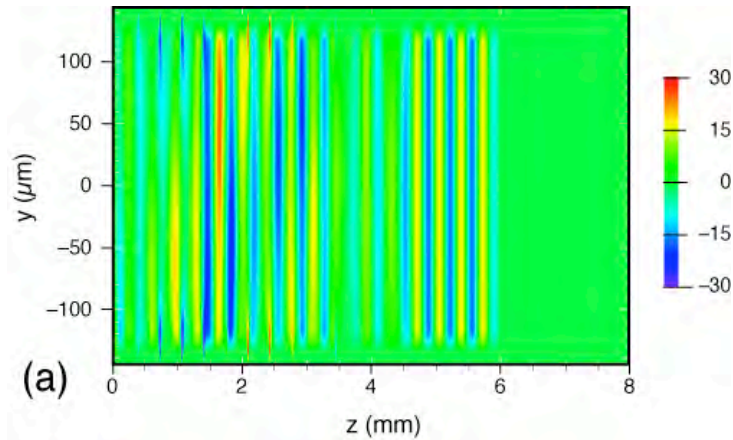


*Longitudinal wakefield*  
(only about 10-50 kV/m, depending  
on beam  $\sigma_z$ , charge)



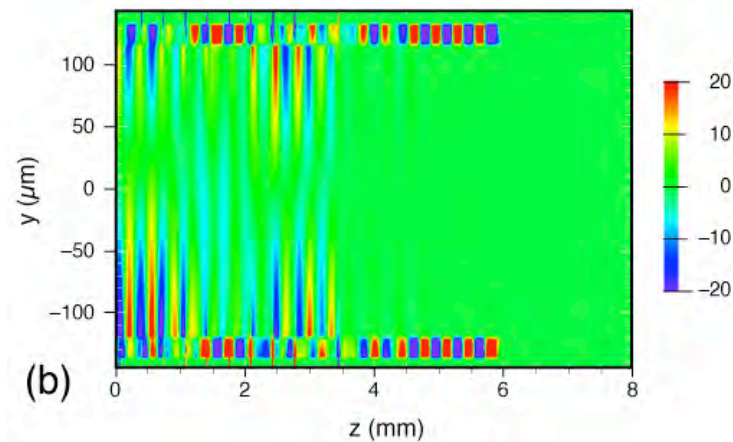
*Transverse wakefield*  
(suppressed in the vacuum region  
for all beams, because of slab  
geometry)

# Wakefields: With slots



longitudinal

(kV/m)



transverse

(kV/m)

- *Fields are altered*
- *Transverse wakes  $\neq 0$*
- *Multimode*
- *Wake sizes still small*
- *Wake group velocities less than  $c$*

# Conclusion

- Laser-driven structure analysis must include **consideration of the coupling**
- **Distributed side-coupling seems advantageous** in view of the damage limits on end-coupling

## *Slot-coupling scheme:*

- Slot dimensions control fill and axial field
- High fields: possible breakdown limit
- Resonant frequency perturbation: design must be adjusted
- Slots do not cause energy loss or strong perturbation, but
- Slots add multimode component to wakefields



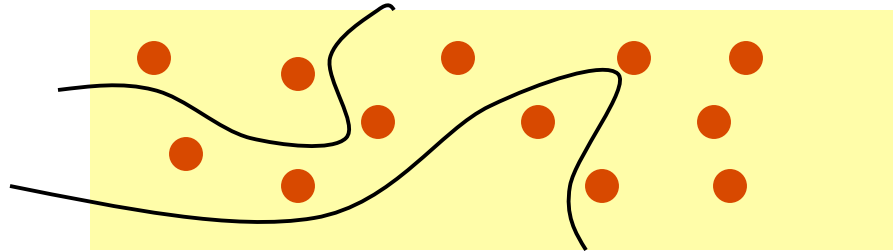
*CHANNELING projects at LNF:  
From Crystal Undulators to Capillary Waveguides*

*Sultan Dabagov, Massimo Ferrario, Luigi Palumbo and Luca Serafini*

*PAHBEB - 2005, Erice, 13 October 2005*

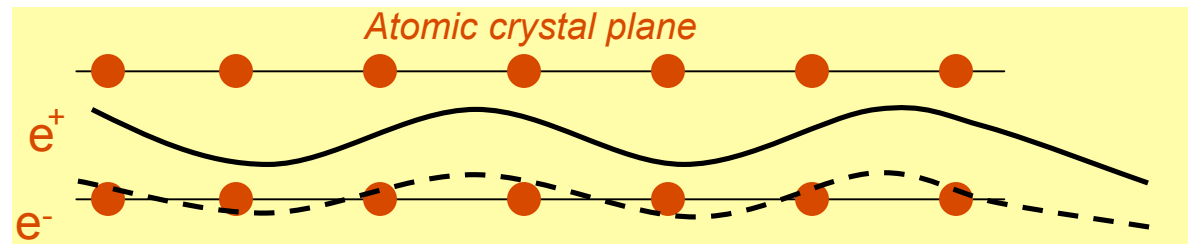
# Channeling of Charged Particles

@ Amorphous:

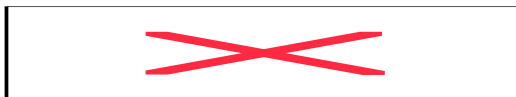
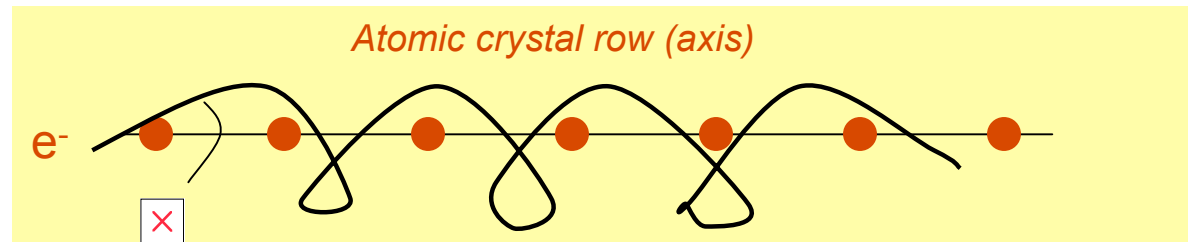


@ Channeling:

planar channeling



axial channeling



- the Lindhard angle is the critical angle for channeling

# Potentials: Doyle-Turner approximation

$f(\mathbf{k}) = 4\pi Ze \sum_{j=1}^N a_j \exp(-k^2/4b_j^2)$  - form-factor for the separate fullerene

$V_R(\rho) = (4Ze^2/d_R) \sum_{j=1}^N a_j b_j^2 \exp(-b_j^2 \rho^2)$

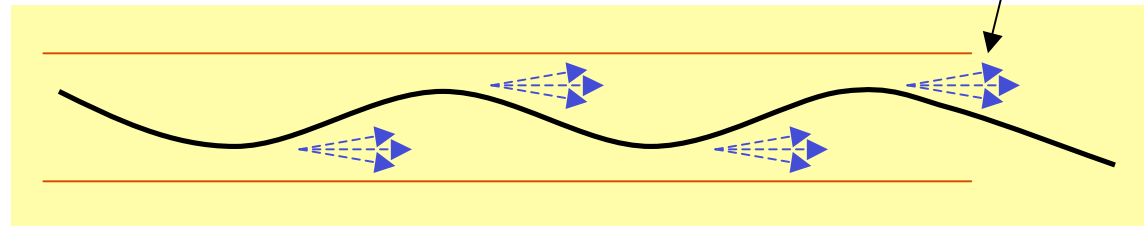
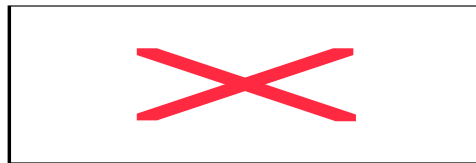
$U(\mathbf{r}) = \sum_i V_R(|\mathbf{r} - \mathbf{r}_i|)$  continuum potential  
 as sum of row potentials

$U(r) = (16\pi dZe^2/3\sqrt{3}l^2) \sum_{j=1}^N a_j b_j^2 \exp\{-b_j^2[r^2 + (d/2)^2]\} I_0(b_j^2 rd)$

$r$  - distance from the tube  
 $I_0(x)$  - mod. Bessel function

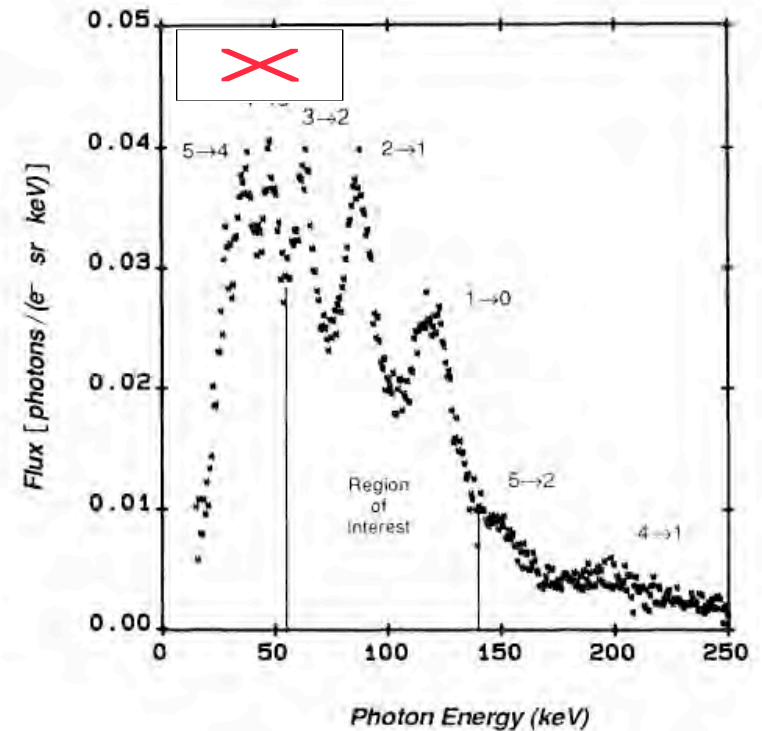
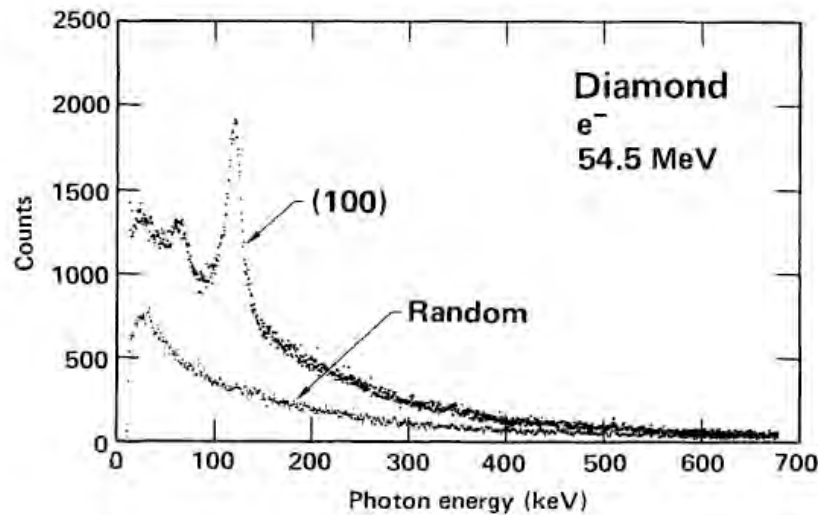
# Channeling Radiation...

@ Channeling Radiation:

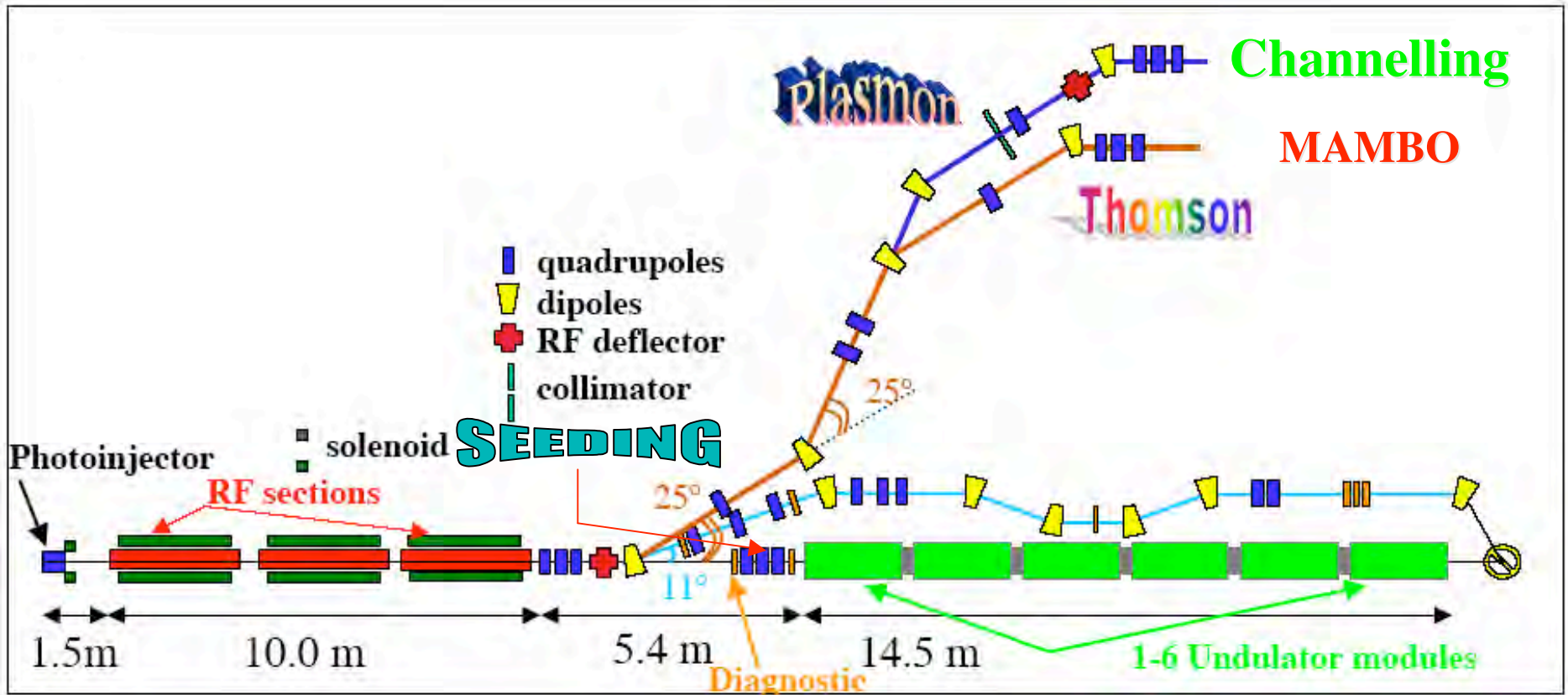


Powerful radiation source of X-rays and  $\gamma$ -rays:

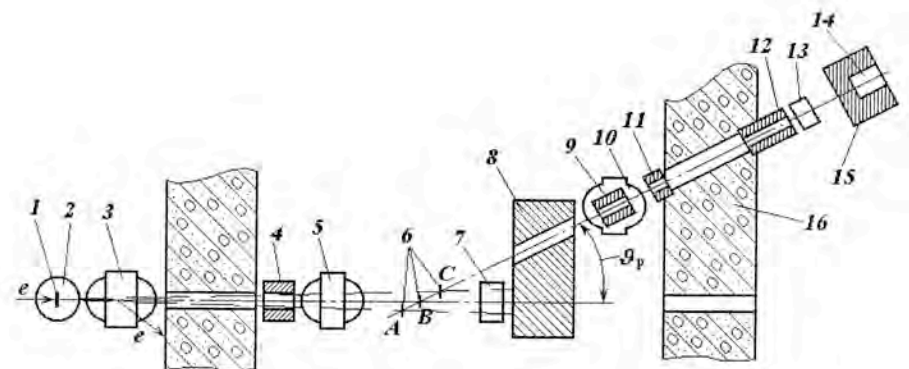
- polarized
- tunable
- narrow forwarded



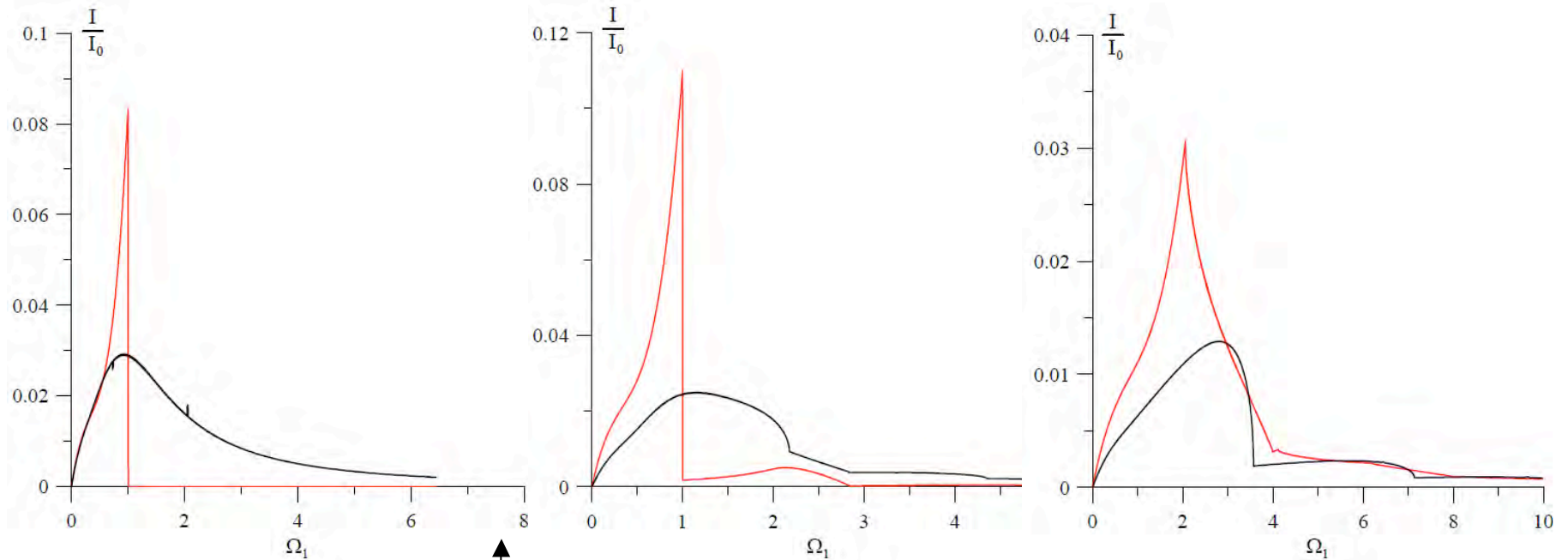
# Experimental scheme



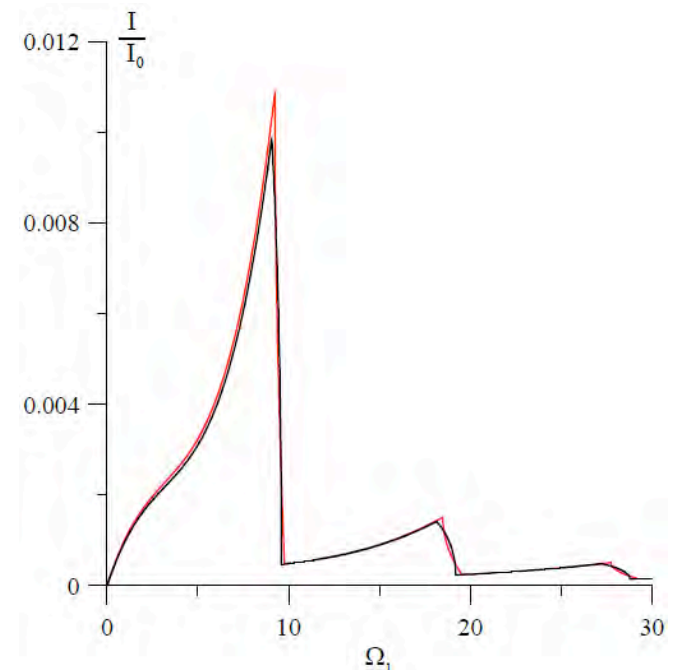
“Channeling” line layout  
by Kharkov group



# Calculation of ChR spectra



Channeling Radiation  
VS  
Coherent Bremsstrahlung



# Summary of LPWA and New Schemes

1. **Generation of monoenergetic electrons** from a laser plasma cathode and the future applications for **pulse radiolysis, Thomson scattering X-ray generation, and electron microscopy.**  
(Kinoshita(Univ.Tokyo))
2. Preliminary Results from the UCLA/SLAC **Ultra-High Gradient Cerenkov Wakefield Accelerator Experiment.** (Travish(UCLA))
3. Coupling Laser Power into a **Slab-Symmetric Accelerator** Structure.  
(Yoder(Manhattan College))
4. **CHANNELING** projects at LNF: From Crystal Undulators to Capillary Waveguides. (Sultan Dabagov(INFN))

Thank you very much for cooperation and nice discussion  
to all contributors and participants.

Applications of High Brightness Beams  
gives

Many important subjects to be solved,  
but also,

**Many Dreams !!**

**Grazie!**

**ありがとうございます！！**